REPORT DOCUMENT PAGE

Form Approved
OMB NO. 0704-0188

1. AGENCY USE ONLY (*LEAVE BLANK*)	2. REPORT DATE	3. REPORT TYPE AND DATES COVERED
	January, 2002	Final Progress Report Grant Extension August 1998 – December 31,2001

4. TITLE AND SUBTITLE
Lateral Migration Radiography Application To Land Mine Detection, Confirmation and Classification

5. FUNDING NUMBERS
ARO Grant
DAAG-55-98-1-0400

6. AUTHORS
Edward T. Dugan
Alan M. Jacobs

7. PERFORMING ORGANIZATION NAMES(S) AND ADDRESS(ES)
Department of Nuclear and Radiological Engineering
202 NSC, P.O. Box 118300
University of Florida
Gainesville, FL 32611

8. PERFORMING ORGANIZATION REPORT NUIMBER
38830.7-MA-LMD

9. SPONSORING / MONITORING AGENCY NAME(S) AND ADDRESS(ES)
U.S. Army Research Office
P.O. Box 12211
Research Triangle Park, NC 27709-2211

10. SPONSORING / MONITORING AGENCY REPORT NUMBER
Proposal NO. 38830-MA-LMD

11. SUPPLEMENTARY NOTES
The views, opinions and/or findings contained in this report are those of the author(s) and should not be construed as an official Department of the Army position, policy or decision, unless so designated by other documentation.

12A. DISTRIBUTION/AVAILABILITY STATEMENT
Approved for public release; distribution unlimited.

13. ABSTRACT
Lateral migration radiography (LMR), a new form of Compton backscatter x-ray imaging, is applied to the detection and identification of buried land mines. Uncollimated detectors provide images that are due primarily to single-scatter photons from the soil surface or near-surface. Collimated detectors provide images that are due primarily to multiple-scatter photons from the near-surface or sub-surface.

Noise removal and image enhancement techniques including simple weighted filters, Weiner filters, optimal filters and neural networks have been successfully employed on LMR images. Information from both the uncollimated and collimated detector images is used to effectively remove surface clutter and enhance mine detection and identification.

An innovative rotating collimator for the x-ray source has been developed to provide rapid side-to-side scanning of the source beam without having to move the x-ray generator in this direction. Acquisition of detailed images of a 40 cm by 40 cm area takes from 30 to 60 seconds, depending on desired resolution.

The construction and testing of a portable LMR system for out door mine detection was completed. This system includes the x-ray generator; rotating source collimator; large area scintillator detectors; system frame assembly; motors and sensors for side-to-side and front-to-rear scanning; x-ray generator scan and data acquisition and processing systems; a standoff-to-vehicle IR modem communication system; and a portable electric generator power system.

System weight (not including the vehicle) is about 160 kg, but this initial portable system was significantly over-designed; system weight for a prototype should be in the range of 100 kg. X-ray generator power requirement is from 200 to 800 watts. This portable system successfully acquired images of mines buried in an indoor soil box and then in out-of-door tests. Very good image results were obtained when the system was employed on the vehicular test lanes at Fort A.P. Hill in Virginia in October, 2001

14. SUBJECT TERMS	15. NUMBER IF PAGES
LANDMINE DETECTION, COMPTON BACKSCATTER X-RAY IMAGING, LATERAL MIGTRATION RADIOGRAPHY, IMAGE PROCESSING, SURROGATE BURIED LAND MINES, LANDMINE CONFIRMATION SENSOR, LAND MINE IDENTIFICATION	16. PRICE CODE

17. SECURITY CLASSIFICATION OR REPORT	18. SECURITY CLASSIFICATION OF THIS PAGE	19. SECURITY CLASSIFICATION OF ABSTRACT	20. LIMITATION OF ABSTRACT
UNCLASSIFIED	**UNCLASSIFIED**	**UNCLASSIFIED**	**UL**

Lateral Migration Radiography Image Signatures for the Detection And Identification of Buried Land Mines

Grant Extension
Technical Report
ARO Grant Number
DAAG-55-98-1-0400

By

Edward Dugan
Alan Jacobs

Additional Report Contributors

Dan Ekdahl
Laurent Houssay
Zhong Su

NUCLEAR AND RADIOLOGICAL ENGINEERING DEPARTMENT
UNIVERSITY OF FLORIDA
Gainesville, FL 32611
January, 2002

Abstract

Lateral migration radiography (LMR), a new form of Compton backscatter x-ray imaging, is applied to the detection and identification of buried land mines. Uncollimated detectors provide images that are due primarily to single-scatter photons from the soil surface or near-surface. Collimated detectors provide images that are due primarily to multiple-scatter photons from the near-surface or sub-surface.

Noise removal and image enhancement techniques including simple weighted filters, Weiner filters, optimal filters and neural networks have been successfully employed on LMR images. Information from both the uncollimated and collimated detector images is used to effectively remove surface clutter and enhance mine detection and identification.

An innovative rotating collimator for the x-ray source has been developed to provide rapid side-to-side scanning of the source beam without having to move the x-ray generator in this direction. Acquisition of detailed images of a 40 cm by 40 cm area takes from 30 to 60 seconds, depending on desired resolution.

The construction and testing of a portable LMR system for out door mine detection was completed. This system includes the x-ray generator; rotating source collimator; large area scintillator detectors; system frame assembly; motors and sensors for side-to-side and front-to-rear scanning; x-ray generator scan and data acquisition and processing systems; a standoff-to-vehicle IR modem communication system; and a portable electric generator power system.

System weight (not including the vehicle) is about 160 kg, but this initial portable system was significantly over-designed; system weight for a prototype should be in the range of 100 kg. X-ray generator power requirement is from 200 to 800 watts. This portable system successfully acquired images of mines buried in an indoor soil box and then in out-of-door tests. Very good image results were obtained when the system was employed on the vehicular test lanes at Fort A.P. Hill in Virginia in October, 2001

Table of Contents

Statement of Problem Studied

A series of buried landmine detection measurements using a novel x-ray Compton backscatter imaging (CBI) method were performed at the University of Florida in 1998 using 12 actual antitank and antipersonnel mines. These tests were conducted indoors using a soil box and an old x-ray therapy machine for the x-ray source. The resulting images were stunning in their definitive detail. The signatures were so unique, that it was apparent that this approach could provide not only for reliable mine detection, but also for mine type identification. The mine's exterior shape, combined with the interior air volumes yield vivid, easily recognized signatures. The image data provides information on the mine size and shape, (x, y) location and depth-of-burial (DOB).

The new CBI method developed at the University of Florida and used to obtain the signatures of the live mines has been given the name lateral migration radiography (LMR). Unlike conventional CBI techniques which utilize only single-scatter photons, LMR uses both multiple- and single-scattered photons. LMR requires two types of properly configured detectors. Uncollimated detectors image primarily single-scatter photons while collimated detectors image predominately multiple-scatter photons. This allows for the generation of two separate sets of images, one containing primarily surface or near-surface features and the other also containing subsurface features. These two image sets make LMR useful for imaging and identifying objects to depths of several x-ray photon mean free paths (~10 cm) even in the presence of surface clutter.

The first task under this work was the purchase of a compact, high intensity, state-of-the-art, low-noise, DC x-ray generator to replace the old x-ray therapy machine. A related task was to develop special, large area scintillator detectors, including special compact photomultiplier tubes and associated electronics and combine these with the new x-ray generator to obtain an efficient LMR imaging system. A second task was to construct simulated or dummy mines that accurately mock up the internals of actual mines, including especially void spaces. Commercially available dummy mines, developed primarily for E&M methods, were poor surrogates for the LMR method because the casing materials used did not have a good match in atomic number, or Z, with the materials in actual mines.

The next task was to determine the effect of the angle of incidence with the soil of the x-ray source beam on mine signatures and image quality. Some of the work with the actual mines suggested that having the source beam strike the soil at an angle different than 90 $^{\circ}$ could lead to enhanced images and to increased DOB for mine detection. To expedite this evaluation, Monte Carlo simulations were to be performed, in conjunction with experiments, to determine these effects. Experiments and Monte Carlo simulations were also to be used to establish limits and conditions under which LMR signatures can be used to detect and identify buried land mines.

An important task of this research was to develop an image processing approach or hierarchy for utilizing the multiple sets of LMR images for mine detection. A related task was the development of specialized LMR image processing, enhancement and target recognition algorithms. As a proof of principle of mine detection with LMR, a final task was the construction and testing, out-of-doors, of a portable LMR land mine detection system. The resulting system was called the X-ray Mine Imaging System (XMIS). Very good image results were obtained when the system was employed on the vehicular test lanes at Fort A.P. Hill, Virginia in October, 2001.

Introduction and Background

Development of the imaging concept to detect buried land mines used in the present work began when Fort Belvoir personnel proposed to the University of Florida (UF) that a particular variant of x-ray Compton backscatter imaging (CBI) be applied to the extraordinarily difficult problem of buried, plastic land mine detection. The technique which we had developed for medical applications produced tomographic images of electron density and atomic number variation on a plane lateral to the incident x-ray illumination direction and with controllable, variable depth from the object surface. However, it was clear early in the project that the method, designed for medical and industrial diagnostics, was not directly applicable to the mine detection problem. Specifically, the desired image data acquisition rate for the land mine detection application implies detection efficiency for relevant, information bearing photons which is orders-of-magnitude higher than the previously developed CBI technique, or for that matter, far greater efficiencies than any other CBI approach. In response to this dilemma, we developed a totally new CBI approach which we have designated lateral migration radiography (LMR).

A CBI system operates somewhat like an optical visual system where the reflected photons from surfaces of the objects are employed to form an image of the object. All existing CBI systems rely on penetrating photons (x-rays or gamma rays) which have had only a single scatter in the object to form an image. Object surface irregularities and internal inhomogeneities obstruct and corrupt such first-scatter dependant techniques. Highly localizing collimators on both x-ray generator and scatter field detectors, as well as slow-running, complex image data algorithms are required to extract useful subsurface structure information. This leads to high source strength and slow imaging system operation.

The technique of LMR is a new imaging modality developed at UF [1-20] which uses the lateral transport of both single and multiple scattered photons to form separate images. Large area detectors operating in the current or integration mode rather than in the voltage or counting mode help to reduce the required x-ray source strength and image acquisition time. LMR systems use two types of detectors to form images. Uncollimated detectors sense predominantly first-collision photons and primarily generate images of surface or near-surface features. Properly positioned collimated detectors sense predominantly multiple-collision photons. The contrast in the collimated detector images is due to multi-scattered photon lateral transport which is sensitive to the electron density of the transport medium as well as the surface spatial details. This enables us to image, with high photon collection efficiency, objects that contain clusters of subtle imperfections and discontinuities in electron density and identify such electron density differences. The multiple-collision photons always carry the information of the first collision. However, with the increase in the number of collisions, multiple-collision components average out small-sized electron density variations while retaining the information from the large-size discontinuities. Because the LMR images are no longer restricted to first-scatter photons, this modality is useful for imaging objects even in the presence of surface clutter with high photon detection efficiency.

An objective of the research for this program was to arrive at an LMR system concept and preliminary design, which could yield a compact, field-deployable unit. This objective was achieved and reported and is reported herein. This LMR system design includes an x-ray generator with articulating collimator, three x-ray detector panels, a computer with a data acquisition board and display, digital control electric motors to provide articulation and positioning, and an electric power generator all mounted on a suitable vehicle platform. The resulting system has been named X-ray Mine Imaging System (XMIS).

In the next section of this report the components of the XMIS are identified and described, along with relevant specifications for this application. The physical configuration of the set of components and the description of information flow among the components to enable operation is also described. Further following report sections contain details of the electronic/electrical components, the image acquisition and display choices and algorithms, and the results of a field test at Fort Hill, Virginia performed as the culminating task of evaluating the XMIS.

The X-ray Mine Imaging System

The X-ray Generator

For XMIS, the forced-air-cooled version of the LORAD LPX-160 constant potential X-ray generator provides an excellent source from the standpoint of performance, size and weight. The LPX-160 is a rugged, commercial X-ray tube designed for field inspections or pipe welds. The LPX-160 has a maximum x-ray spectrum energy of 160 kVp and a maximum power level of 800 watts. The optimum x-ray source energy for the detection of mines with backscattered x-rays is in the range of 120 kVp to 160 kVp. Good imaging quality requires about two million source x-rays per pixel and this translates into an electric energy requirement of one joule per pixel. A pixel size of 15 mm by 15 mm provides good resolution for both antitank and antipersonnel mines and for image scan times on the order of 10 to 100 seconds, the required x-ray generator power level is found to be 100 to 200 watts. The weight of the air-cooled LPX-160 tube head is 15 kg and the weight of the control unit is 16 kg. The tube head is 18.4 cm in diameter and 77.5 cm in length. The control unit is 30.5 cm by 26.7 cm by 45.7 cm.

The X-ray Generator Collimator

A significant accomplishment in this research effort was the development of an x-ray source collimator design that uses a continuously rotating cylinder to synthesize a moving aperture from side-to-side with negligible retrace time. Coupled with the x-ray generator forward motion, this provides a raster scan of the ground. This collimator design is a key element in reducing the required x-ray head movement and in obtaining a simple, compact LMR detector system. Although this collimator efficiently achieves raster direction side-to side motion while delivering the same photon intensity to each pixel, it results in the x-ray source beam having an incident angle that is perpendicular to

the ground only at the central location in the scan. This source beam tilting causes a raster direction distortion in the acquired images but this slight distortion is readily removed by using simple geometric projection. A photograph of the air-cooled LPX-160 and the fabricated x-ray generator collimator assembly is included as Figure 1 in which the size scale is apparent by noting that the diameter of the cylindrical collimator assembly is about 30 cm and the length of the generator is approximately 78 cm .

Figure 1. The LORAD LPX-160 and the rotating x-ray source collimator.

X-ray Detector Array

Careful detector design and deployment are critical for proper functioning of the LMR mine detection system. High performance organic scintillator block detectors from Bicron, Inc. are used for both the collimated and uncollimated detectors in the XMIS. The uncollimated detector is 140 cm long, 5 cm wide and 2.5 cm thick. The collimated detectors are 140 cm long, 20 cm wide and 2.5 cm thick. The detector collimators are made from 1.5 mm thick lead sheets. Photomultiplier/amplified/bias-voltage-supply assemblies provide signal amplification and serve as the output device for each of the three plastic scintillator detectors. The photomultiplier tubes attach to the ends of the detectors. The weight of the detector assemblies, including the housing and collimators, is about 30 kg.

Configuration of the LMR System Components

Figure 2 illustrates the relative positioning of the LMR components of the XMIS. The x-ray generator with rotating collimator assembly is supported above, and fixed relative to, the mounting platform, which is a 1.9 cm thick aluminum plate. Attached, and fixed relative, to this platform are the detector panel array supports, the digital electric servo motors (not shown in the figure) which provide rotational motion to the x-ray collimator through a belt drive and translational motion to the platform through a lead screw (both not shown in figure), and linear ball bearing assemblies (not shown in figure) which support translational motion (left-to-right in the figure) of the platform. The linear bearings surround two cylindrical steel rails (length left-to-right, but not shown, in the figure). These rails are fixed to the rigid steel frame structure which also provides fixed relative positioning of the limit and safety switches for the platform linear motion. Figure 3 is a photograph of the LMR system as just described. The linear drive lead screw is visible in the lower right corner of the photograph.

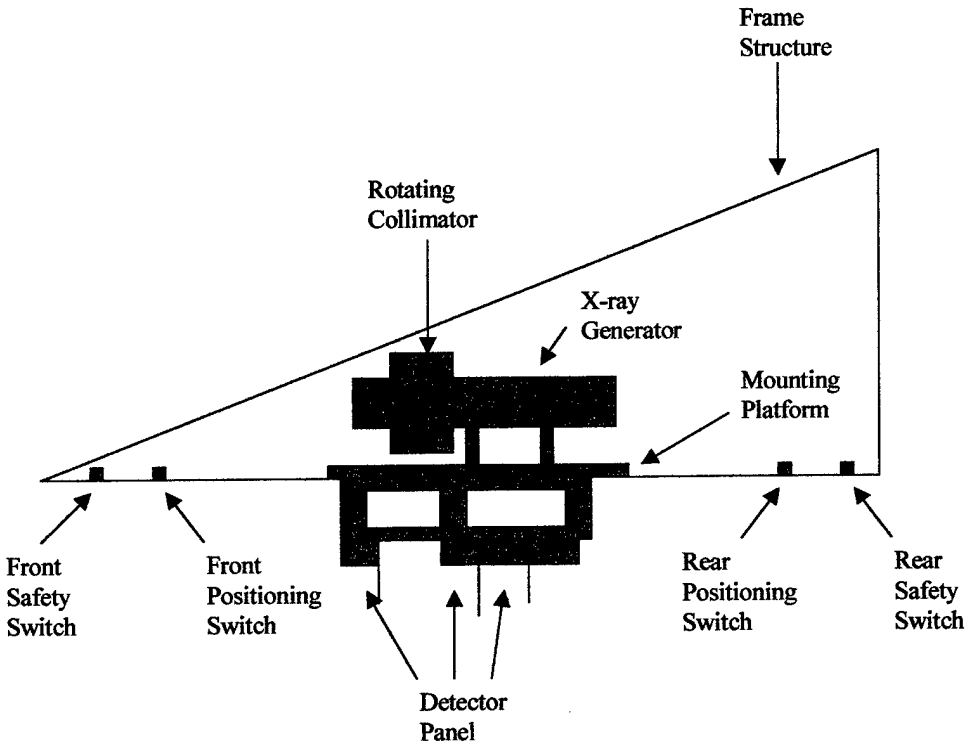

Figure 2. The LMR landmine detection system

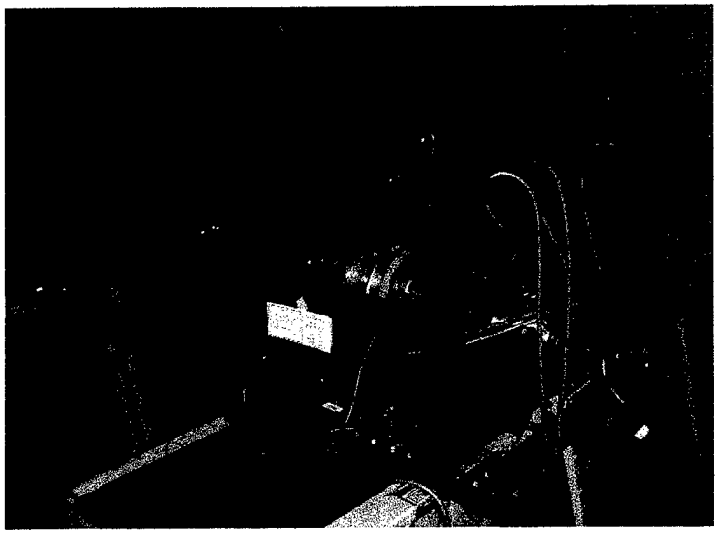

Figure 3. The LMR land mine detection system before XMIS installation

In Figure 4 the mechanical and electrical interrelation of the XMIS components is illustrated. The components, which were not identified in the LMR system description, are electrical power and electronic control equipment for the XMIS. They are described completely in a later section of this report.

The XMIS Vehicle

The weights of the LMR system components are summarized in Table 1. The forklift extension channels have not been discussed to this point. They are included in Table 1 to provide for a suggested capability that an LMR land mine detection vehicle should be relatively agile in field positioning. These, rather heavy, structural parts are included in the XMIS design, but the XMIS did not actually employ their function, which is to facilitate a forklift vehicle support of the LMR system.

Table 1: LMR System component weights.

Aluminum platform and lead shielding	35 kg
Detector array assemblies	30
Unistrut steel frame structure	28
Fork lift extension channels	27
X-ray generator & control/power supply	31
Cylindrical steel rails	11
Servo motors & steel lead screw	8
Rotating collimator assembly	5
Total	175kg

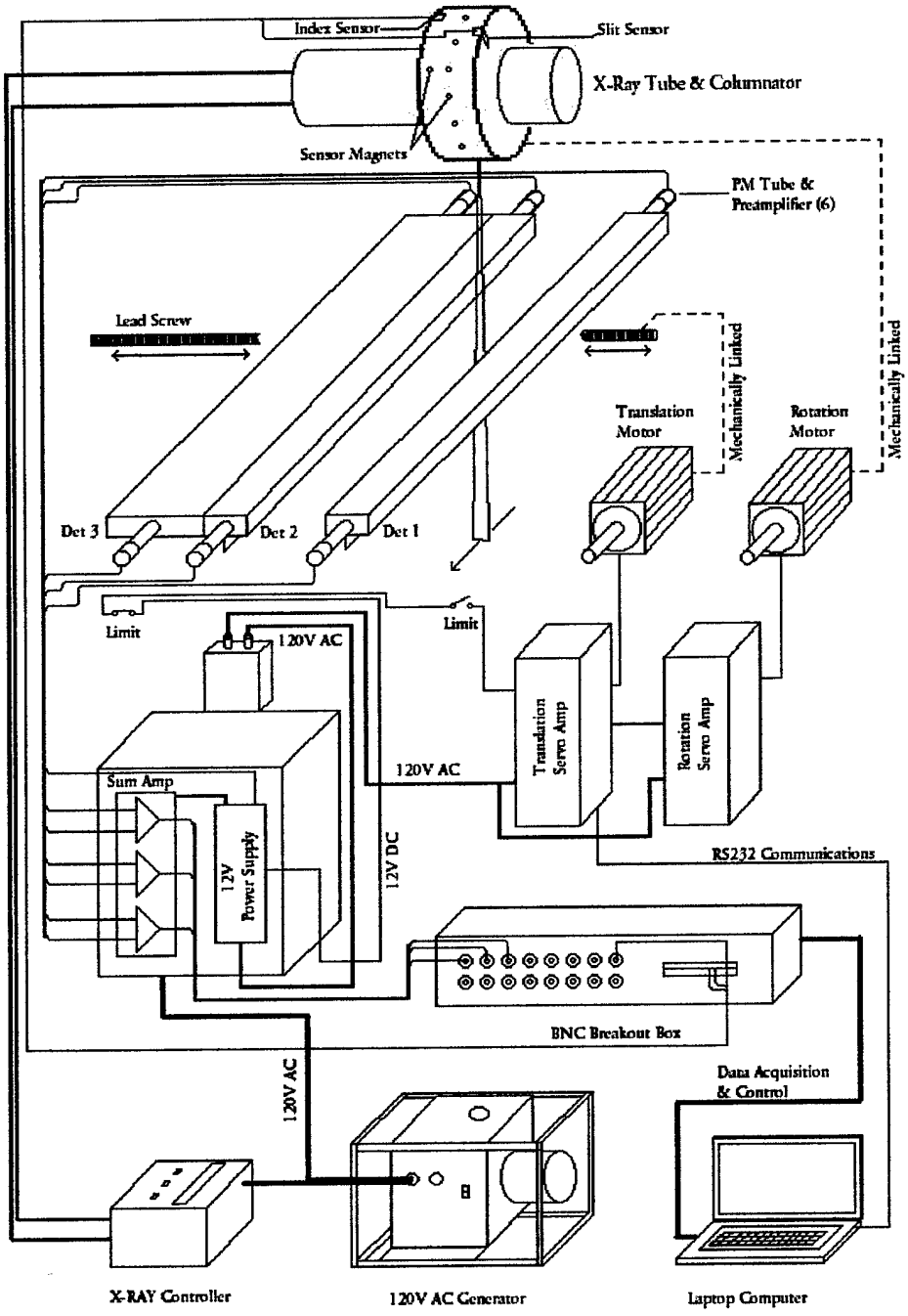

Figure 4. XMIS components interrelation and information flows.

In order to provide a vehicle which would serve the dual function of easy delivery to the Fort A.P. Hill test site, and performance of the anticipated testing procedures, we chose to mount the LMR systems aft of the axel of a boat trailer-like vehicle designed and fabricated specifically for this purpose. The overall dimensions of the trailer are about six meters long (including tong assembly) and about 2.3 meters wide (including the tires). The rear open bay over which the LMR systems is positioned is approximately two meters in the trailer length direction and 1.75 meters in the trailer width direction. Four screw jacks fixed to the trailer frame at the corners of this rear bay provide for adjustment of LMR system height and leveling relative to the ground. Figure 5 is a photograph of the XMIS showing the LMR system mounting relative to the trailer rear bay. This photograph was taken at Fort A.P. Hill in a preparation garage shortly after the system arrived. The x-ray generator is in position, but the detector array assembly has not yet been attached. One of the (yellow tipped) forklift extension channels is in the picture foreground. The (green) fabric cover for protection during transit, and sunshade during operation, is at the picture top. Figure 6 is a photograph of XMIS in position for a land mine image acquisition on a gravel land mine lane. The (yellow) motor-generator, which provides electric power for all LMR components, is shown at the front of the trailer, i.e., the right side of the photograph. One of the aluminum-clad lead-sheet, detector collimators is clearly visible in the photograph as the LMR system component closest to the ground. Figure 7 is another photographic view of the XMIS illustrating the position of the system operator with control laptop computer.

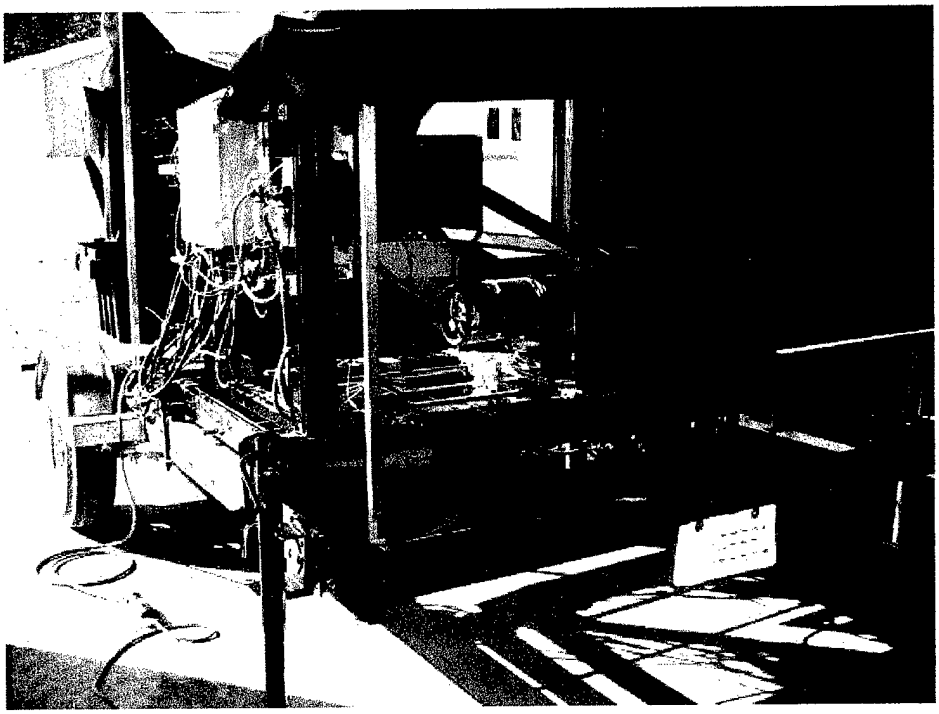

Figure 5. LMR system mounted on the XMIS vehicle.

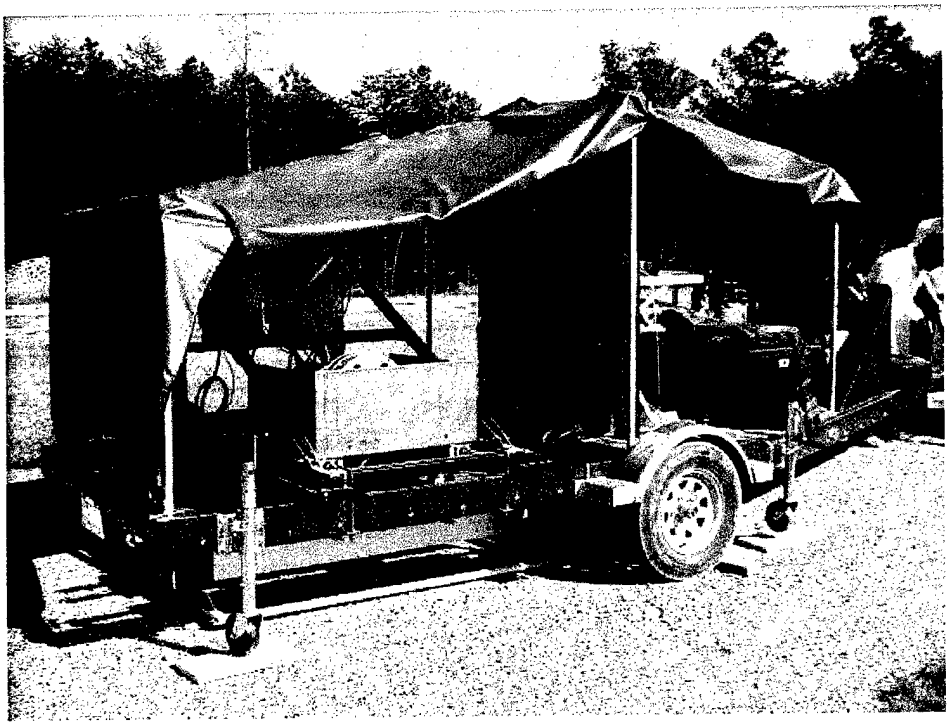

Figure 6. The XMIS in position for image acquisition on mine lane.

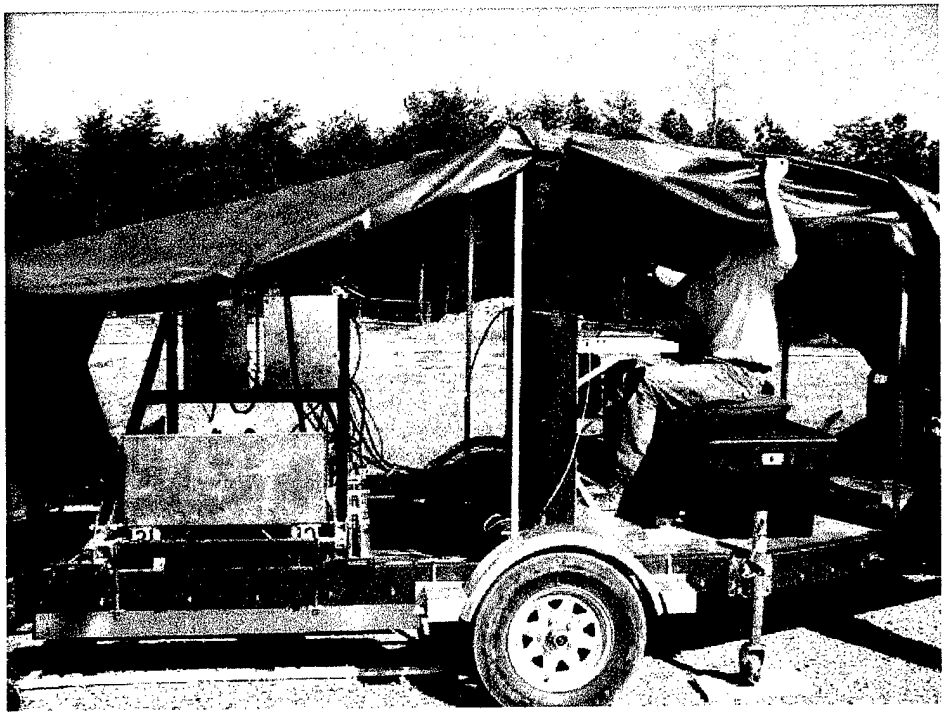

Figure 7. The XMIS with system operator during image acquisition.

The mobile XMIS prototype interrogates a square ground surface area of approximate one-half meter side size. At the Fort A.P. Hill test, the image acquisition time varied from 30 to 60 seconds, depending on the pixel resolution required. For this test the x-ray generator was run at 150 kVp and 5 ma, i.e., an electric power of 750 watts. The product of x-ray generator electric power and image acquisition time interval is about on order-of-magnitude higher than suggested in the final report design concept. This is due, in part, to our desire to assure quantum noise-free images, but is also the result of a far from optimized fit between the Bicron plastic detector x-ray scintillation blocks and the optical photon collection and measuring devices (the photomultipliers), which were chosen because of ease of mating to the Bicron conventional block and because of familiar operation characteristics.

Electric and Electronic Components

In Figure 8 the flow of signals for the LMR system is shown as a block diagram. This diagram, along with the XMIS schematic configuration shown in Figure 4, shows the interrelation of the components discussed in this report section.

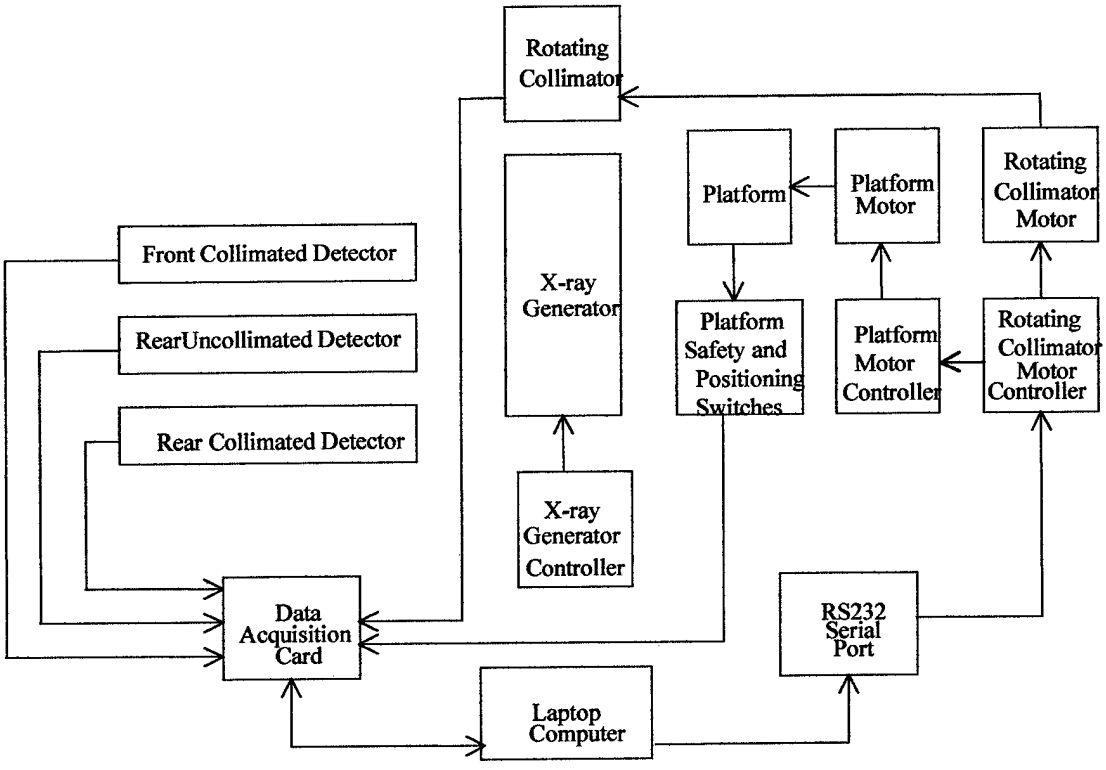

Figure 8. Block diagram of signal flows in the LMR land mine detection system.

Electric Power and Distribution

Electric power (120 v AC) for the entire XMIS is derived from a two-kilowatt gasoline-fueled motor-generator. Fuel capacity is approximately five gallons which is ample to run the mine detection apparatus continuously for eight hours. A breaker on the generator panel switches the mains for the entire system. All connectors are compatible with standard 30 amp 120 v AC electrical trade sizes which allows the mine detection system to be powered by a typical outlet without the gas generator.

Outlet AC power from the gas generator terminates into a distribution box, from which it is distributed to the x-ray generator, control box, and servo amplifiers. Extra outlets from this distribution box also allow for fans, chargers, lighting and other accessories to be added by the operator. The generator's 120 v AC power is converted to 12 v DC to power the various detection related electronics. It is also converted into a 25 kHz square wave drive by the x-ray generator for its own power supply.

System Control Box

The control box has two primary functions: To provide a clean, well-regulated 12 v DC to all the electronics in the mine detector system, and, to house the summing amplifier. The box itself is a NEMA standard enclosure with waterproof gasket seals, a clear protective front panel cover, and water tight cable conduits. The 12 v DC power supply incorporated within the housing is comprised of two high reliability modules from VICOR, Inc. The first module provides a filtered and well regulated 100 v DC to the second module, which is a low ripple 12 v DC regulator. This combination of both AC and DC regulation provides a clean DC power source, which is insensitive to both transients and brown out conditions which may occur in the gas driven generator. This 12 v DC source is used to power all amplifiers, including the detector preamplifiers and summing amplifier and the safety interlocks.

The summing amplifier performs three distinct functions, all of which are used to condition the analog data before being acquired and processed by the computer. The first of these functions is to provide an individual gain adjustment to each of the two signals of either side of each detector assembly. The purpose of this is to balance the two signals received by the photomultiplier tubes on each end. Imbalances can occur for various reasons, such as small differences between photomultiplier tubes, variations in high voltage tube bias assemblies, or small differences in the quality of the optical interface. The second function provided by the summing amp is to provide zero suppression (or DC offset) control to the input signal. Undesired DC level shift in the input signal are typically very small and may come from such sources as electronic offset in the tube preamplifier or from stray x-ray fields not associated with the scanning beam itself. This adjustment allows for a zero voltage baseline in the absence of any real detector signal. The third function of the summing amplifier is to provide an overall gain for the detector signal in order to take advantage of the A/D converter's full dynamic range. This control can also be used to balance each detector assembly against the other two detectors for more uniform signal overall output.

Photomultiplier Tubes, Preamplifiers and High Voltage Supplies

Mounted on either end of each of the three plastic detectors are the photomultiplier tube assemblies, with preamps and bias high voltage supplies. The PM tubes and base assemblies as delivered from Bicron were set up for pulsed voltage mode, so it was necessary to modify the PM tubes to operate in continuous DC current mode for the integral transimpedance type preamplifiers. This modification to the PM tube structure is shown in Figure 9.

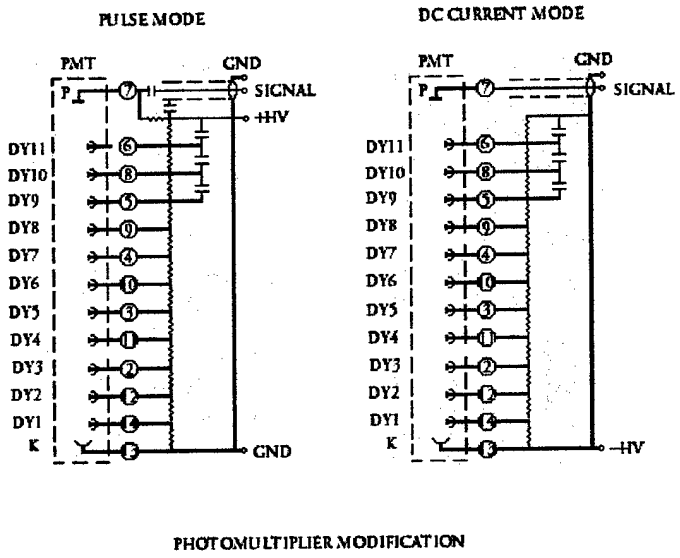

Figure 9. Photomultiplier structure modification.

Design criteria for the transimpedance amplifier were carefully selected to include low input bias current, offset voltage and noise. The amplifier was also designed to perform in a single 12 v DC supply system, as opposed to the more common split supply systems. The transimpedance amplifier, by nature, offers a very low input impedance, which is necessary for current output type sensors. It additionally converts the current signal to a voltage signal for further amplification.

Also housed within the PM tube preamplifier assemblies is the high voltage DC bias supply required to operate the PM tubes. The HV bias supply consists of a HV module manufactured by PICO Electronics, 1.3 cm square on a side, and PC board mountable. Bias voltage adjustment is resistor programmable through a voltage regulator integrated circuit located on the same PC board.

The housing for the preamplifier is specially milled from brass stock and also serves as a low noise faraday shield. An internal divider separates the preamplifier electronics from the bias supply for protection and also for noise immunity. Due to the high sensitivity of the preamplifier's front-end electronics, grounding braids are attached to each of the detector's PM tubes and are ultimately terminated to the gas generator's grounding system. Each PM tube is sealed to protect against light leakage and also to provide protection from moisture intrusion. Figure 10 shows the internal construction of the PM tube preamplifier assembly, and Figure 11 is a photograph of the assembly (tube diameter of about three cm provides picture size scale).

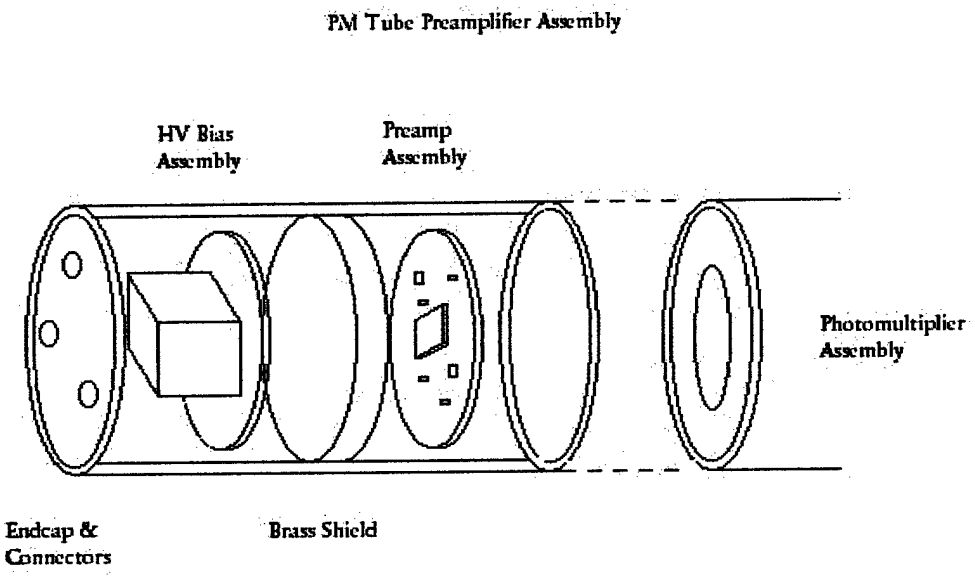

Figure 10. Photomultiplier, preamplifier and high voltage supply assembly.

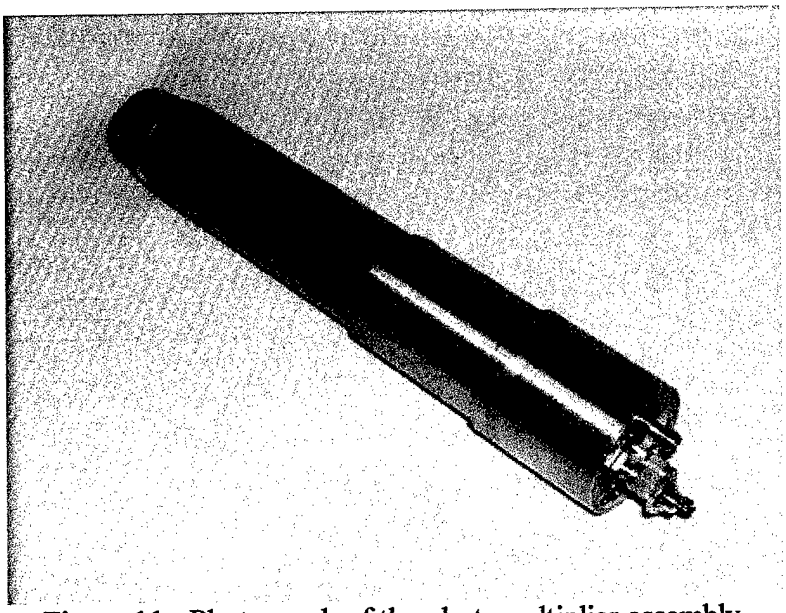

Figure 11. Photograph of the photomultiplier assembly.

Servo Motor Controls

The actual sweep of the x-ray beam is controlled by a dual motor and servo amplifier system manufactured by Kollmorgen called the Servostar System. Commands from the operator's computer are sent to the Servostar system via an RS232 cable. The motors (translational for the forward/ reverse direction and rotational for the rotating collimator) are then pulse-width modulated by the 2 servo amplifiers to control direction and speed of each axis. Each servo amplifier is equipped with resolver feedback sensors with 16 bit resolution for accurate control of it's motor. Motor and mechanical system parameters are initially adjusted and stored through an auto tuning procedure, which is part of the Servostar software. By tuning the servo system in this way, the system automatically compensates for changes in mechanical loading, such as would be experienced by detecting on inclines or other rough terrain. A hard-wired motor enable feature prevents the translation motor from running past it's end play by the use of limit switches.

Magnet Sensors

X-ray beam alignment and control is achieved through the use of magnets and Hall-effect sensors. Two sensors are used; one called index which denotes the start of the entire XY scan, the other references each sweep of the beam and is called slit. Five volt power is provided by the computer via the BNC breakout box, the signal is then returned through the BNC breakout box to one of the digital I/O lines on the acquisition card. Hall-effect sensors were chosen for this task because they are much less sensitive to occlusion caused by environmental conditions than optical sensors are. Built-in signal conditioning within the sensor itself insures that there is no false triggering, or multiple triggered events.

BNC Breakout Panel

The BNC breakout panel provides a convenient interface between the computer and all detector and sensor signals. Additionally, access to all system signals for testing and troubleshooting purposes are obtained at this panel. On the computer side, all analog and digital I/O is combined into a single, shielded cable which easily detaches from the rest of the system thus allowing the use of portable laptop computers for control and image display. The BNC breakout box is itself well shielded for good noise integrity. One modification made to the BNC breakout box was to provide a better connector for the digital I/O, with good insertion force.

LORAD LXP-160 Control Modification

At the manufacturer's recommendation, an adjustment was made to the x-ray generator's control circuitry to make it less sensitive to short transients caused by loading, etc., on the AC generator's power line. This modification in no way affected the safety of personnel or integrity of the mine detection system.

Safety Interlocks and System Interconnects

Whenever the x-ray generator is powered up, a relay automatically energizes for the purpose of providing a safety interlock system to alert personnel that the source is on. Through the set of closed relay contacts in the x-ray generator, 12 v from the control box is supplied to a rotating warning lamp.

All signal and power cabling are provided with quick disconnect type connectors for easy assembly, disassembly, and troubleshooting. Cabling between the moving portion of the landmine detection system and the stationary part are housed in a special umbilical designed especially for highly flexed applications. All connectors are high reliability type with good contact pressure. Military specification connectors are used on the x-ray generator and tube. The next page shows the various system components of the mine detector and their related interconnections.

Image Acquisition and Processing

Data acquisition

Description of the signals

Different types of signals are employed in the system.

> Analog signals: Three radiation detectors deliver analog signals that are treated by three amplification circuits. These signals are positive with amplitudes smaller than 5 v in normal operation.
> Magnet sensors, digital signals: Two digital signals come from two magnet sensors (Hall effect). The Hall effect circuit generates a 0-5 v DC pulse every time a magnet passes by the position of the sensor. This signal is generated for each of the 10 slits of the rotating collimator. Another magnet sensor is used to reference the slits, i.e., mark one of the slits as a starting point. Position switch, digital signal: The last digital signal comes out of a switch that makes contact when the frame is positioned at the back end of the linear range. This signal is also 0-5 v DC and senses when the frame reaches its starting position.

Data acquisition board

Both analog and digital signals are connected to a data acquisition board (DAQ board) through a BNC2090 box. The DAQ board used in this system is the National Instruments DAQCard-AI-16E-4. This fully integrated PCMCIA card processes both analog and digital signals with its internal processors as well as analog-to-digital and timing capabilities. LabVIEW has full control over this card and takes care of the configuration as well as the data extraction. It is setup for non-referenced single-ended bipolar inputs, and a sample rate of 20000 samples per second per analog input. The 5 v and ground reference used by the digital lines are taken from this card. The hardware trigger input of the card is connected to the "slit magnet" signal. Once the card is correctly configured and enabled, any falling edge detected on the hardware trigger input starts a continuous acquisition of a predetermined number of samples on each of the three analog inputs. These samples are automatically transferred to the PC and stored in memory for later processing.

Motor controls

Description of the motors

Two motors activate the mobile parts of the machine. The motor designated "motor 1," is in charge of the movement of the rotating collimator through a belt. The second motor, designated "motor 2," controls the forward/backward motion of the assembly. Each motor has a separate driver that controls its inputs and outputs and its internal parameters.

Communication with the PC

The two motors are fully controlled by a PC through a serial port using a RS232 connection. Many motor parameters are conveniently accessible and can be modified by the PC. The setup of these parameters is accomplished with manufacturer provided software called "motionlink". Once the initial setup is optimized, the "motionlink" software does not control the motors any more. LabVIEW takes over instead and sends

the appropriate string of characters through the serial port of the computer. If the string is sent with the correct format and with the appropriate timing, each motor can start, stop or react "instantly."

Image acquisition

This part describes the chronological steps that result in a set of images. Several programs from the computer automatically execute all the following tasks. These programs are written with LabVIEW which is a graphical-type programming particularly fitted for data acquisition, controls and processing needs.

Pre-acquisition tasks

The initial step is to power up all components of the system from x-ray machine to computer. The main LabVIEW program needs to be opened but not yet executed. The x-ray machine is set up first with the appropriate current, high voltage and time of exposure. These settings are set once and in most cases do not need to be modified later. The x-ray machine can then be started and the main LabVIEW program can be executed.

The following tasks are accomplished in chronological order.

> The serial port link with the motors is initialized and the bi-directional communication tested.

> The position switch is tested. If the frame is not at the desired location, it is moved back until the position switch senses it. The linear motor is stopped when the frame is in its starting position.

> Motor 2 starts and rotates the rotating collimator. The period between two slit magnet pulses is then measured. This value is needed to calculate the number of samples to acquire between two pulses. The sampling frequency is 20000 samples/second and the period is typically in the order of 0.9 s. The computer, however, needs some time to transfer the data from the DAQ card to the memory. Therefore the data acquisition only occurs during the first 85% of the time between two slit magnet pulses. The number of samples to acquire per input is then 20000*0.9*0.85=15300 samples.

> The index magnet signal is tested. When the magnet reaches the detector, linear motor 2 is immediately started and the DAQ board is configured and enabled. The speed of linear motor 2 is calculated depending on the speed of motor 1 and the size of the beam on the ground. There is typically a factor of 13.5 between motor 1 and 2, motor 2 being the fastest

Acquisition tasks

The following tasks are executed every time a magnet reaches the slit magnet sensor that generates a pulse to the hardware trigger.

> About 15300 samples from three analog inputs are automatically acquired and stored in memory.

> Only 73 lines of data can be acquired within the dimension of the frame. The data acquisition is disabled and stopped at the end of the 73rd line.

Post-acquisition tasks

After the data is stored the following tasks are executed
> Motor 1 and 2 are stopped. Motor 2 then moves the frame back to its starting position.
> At this point the data needs to be processed to build a set of images. The basic idea is the following. A color is associated with a value of voltage from each sample. Every group of 15300 samples is a line, and there are 73 lines from bottom to top. The first of the 15300 samples is the pixel on the left, the last one, the pixel on the right. This way it is possible to build an image that has 73 lines of 15300 pixels. If no additional processing is done an image could actually be produced but it would be noisy and stretched out of shape. The image processing applied then on the data is described briefly in the next section
> Once the images are produced they are displayed on the PC monitor. The user has the opportunity to save these images and the data set on the hard-drive for later consultation. An html document is then simultaneously produced to allow a convenient display of the images.

Image processing

The three sets of data from the three detectors are three arrays of 15300 by 73 pixels. This data can be significantly improved by the following techniques. Each of these techniques is described here separately, but is implemented directly in the program.

Pixel integration

The size of x-ray spot on the ground is 1.5 by 1.5 cm when the x-ray beam hits the floor perpendicularly. A line is made of 15300 samples and is equivalent to a distance on the ground of 49.2 cm, i.e. about 33 times the width of the beam. It is obvious here that the 15300 samples can be integrated in order to reduce this number to a more acceptable figure and to decrease the noise simultaneously. For practical purposes, a width of 300 pixels is chosen which yields very good quality image on a computer and does not require too much memory. Each one of these 300 pixels is integrated over the beam width. This pixel is the average over 1/33 of the 15300 samples, that is 466 samples. The new images are then an array of 73 lines by 300 pixels.

Shape correction

The size of x-ray spot on the ground is 1.5 by 1.5 cm when the x-ray beam hits the floor perpendicularly. When the x-rays hit the ground with an angle of 18 degrees, which is the maximum angle allowed by the system, the size of the beam on the ground increases by 10% in one direction. If this effect were not corrected, objects would seem to have shrunk on both sides of the image compared to the center. A shape correction is achieved by integrating each one of the 300 pixels not from 466 samples but from a

continuously varying number of samples close to 466 that would prevent any deformation of shape. This procedure provides the required geometric projection correction.

Delay correction

Each line of an image is made of a series of 15300 samples acquired when a magnet sensor emits a pulse to the hardware trigger of the DAQ board. Very small variations in the position of the magnet relatively to the slit between the ten slits result in poor alignment in one direction. Therefore a delay must be added to the lines in order to keep a good alignment. A delay is in fact equivalent to start the pixel integration not with the first of the 15300 samples but with n^{th} one. This number n is periodic with a period of ten because there are ten slits. The results are shown in Figures 12 and 13.

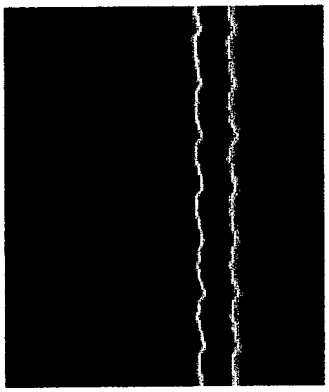

Figure 12. Image of "line" object before delay correction

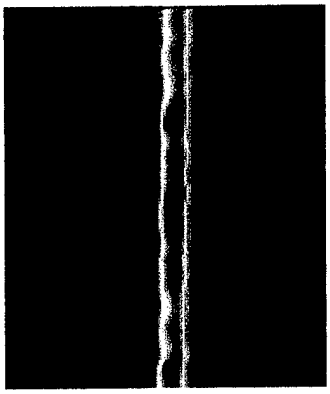

Figure 13. Image of "line" object after delay correction

Normalization

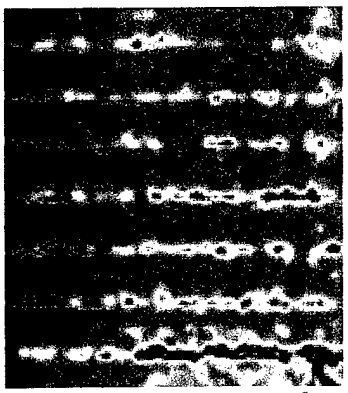

Figure 14. Image of homogenous object.

The flux of photons from the beam of x-rays that hits the ground should be constant but it is not. The flux coming out of the x-ray machine is very much angular dependant. In addition, the dimensions of the slits are not identical. This inhomogeneous field results in significant variations of the detected intensity, even if the ground material is homogeneous as illustrated in Figure 14. One way to fix this problem is to compensate for the intensity variations. The first step is to get an image of a clear, nice and flat area of homogeneous material; this is called the background image. Second, a correction matrix is calculated by replacing each element of the background array by its inverse, once the array has been normalized to unity. Third, any new image has its element multiplied by the corresponding element of the correction matrix. This way the variations of the incident fields are corrected by software, as shown in Figures 15 and 16.

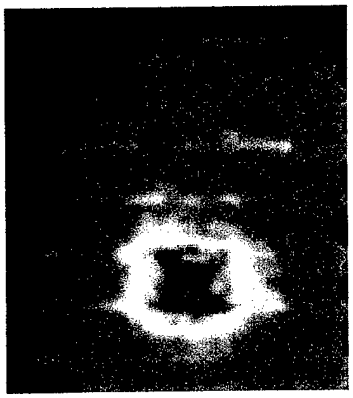

Figure 15. Buried landmine image before normalization matrix correction.

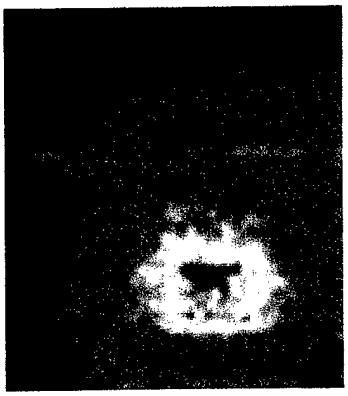

Figure 16. Buried land mine image after normalization matrix correction.

Cross-correlation of images

Three images are available to the user: two collimated images that show surface and buried features and one uncollimated image that shows only near-surface features. A first step is to subtract the normalized uncollimated data from the two collimated data. This technique removes surface objects and provides a better contrast for buried objects. For metallic mines that show as low intensity areas, a sum should be computed instead of a difference. The next technique is a very powerful way to enhance image quality. Any buried object featured on both collimated images does not show at the same location in the image. The positions are shifted in one direction. When one image is shifted against the other, the location of the buried object on both images matches for some shift value. At this point the contrast is greatly improved if the two collimated images are multiplied. The example shown in Figure 17 shows the quality of improvement from this technique.

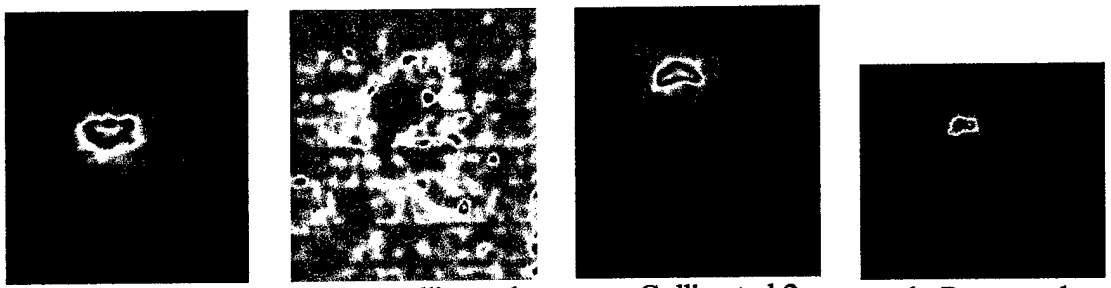

a. Collimated 1 b. Uncollimated c. Collimated 2 d. Processed

Figure 14. Example Application of the image enhancement algorithm.

Image filter

At this point, an image is a set of 73 lines of 300 data points that represents an image 54.8 cm long by 49.2 cm wide. The data is then interpolated in order to give the appropriate aspect ratio to the image: 300 pixels wide by 334 pixels long. Finally a Wiener filter is applied to smooth out the resulting image.

Summary of Imaging Results from Tests at Ft. A.P. Hill

Image sets obtained on the test lanes at Fort A.P. Hill using the XMIS Lateral Migration Radiography landmine detection system are included in the attached Appendix. Each of three separate detectors acquire three separate images. The front and back collimated detectors obtain images formed primarily from multiple scattered photons. These photons contain both subsurface and surface information. The uncollimated detector forms an image primarily from single-scatter photons; these photons contain surface or near surface information. A primary function of the uncollimated detector data is for removal of surface clutter from the collimated detector images. The processed image has had standard digital filtering applied to a cross correlation between the front and back collimated detector images following surface clutter removal by use of the uncollimated detector data.

The LMR imaging capabilities make this system well-suited for use as a mine detection confirmation sensor. To this end, about 30 locations were selected on one of the test lanes at Ft. A.P. Hill where GPR has consistently yielded false alarms. These sites were imaged with the LMR mine detection system. Only six of these locations yielded signatures that had any mine-like features, and in only two cases does the image set indicate a possible mine.

The time required to acquire an image for a ~50 cm x 50 cm area is ~30 s for low resolution and ~60 s for high resolution. This is also the time during which the x-ray generator is actually on. The x-ray generator power level used for these image sets was ~750 watts. The front and rear collimated and uncollimated detector images are acquired real time. The time required to obtain the processed image is from one to two minutes.

When viewing the images, the color scheme designation for regions of highest signal intensity to regions of lowest signal intensity is white, red, yellow, green, light blue, dark blue and purple.

Conclusions and Recommendation

The imaging results obtained at Fort A.P Hill with the XMIS were very good and clearly demonstrate the excellent capabilities of this system as a confirmation sensor for land mine detection. These field tests showed that a series of modifications, some fairly simple, could significantly improve the performance of the XMIS.

Following shipment of the XMIS from the University of Florida to Fort A.P. Hill, reassembly and testing of the system showed light leaks in all three of the detectors. The organic scintillator detector blocks are encased in a protective aluminum clad. Some small separations at the seams along the edges and a few small dimples in the very thin layer of aluminum on the bottom face of the detector during shipment and handling and during operation in the field resulted in the light leaks which had to be repaired.. A more rugged design for the aluminum casing can eliminate these problems.

The thickness of the scintillator detectors could be reduced by a factor of two. The XMIS was designed to provide a 40 to 50 cm wide scan; the very long detector length of 140 cm was used to prevent "edge" effects in the scanned area image. The field testing showed that the detector length could be reduced by 30 % to 40 % without adversely affecting image quality. These changes would yield a reduction in weight of the detector assemblies from 30 kg to under 10 kg. Except for the bottom face, the detector assemblies are each wrapped in lead shielding and the lead collimators on the collimated detectors run the length of the detectors. The indicated reduction in detector size would lead to a reduction in the amount of detector lead and an additional weight savings.

Lead shielding is also used around the x-ray generator to reduce "leakage" radiation from the generator. Such leakage can adversely affect image quality and also increase personnel exposure. A different design for the x-ray generator assembly can reduce the leakage radiation. While this change will increase the weight of the x-ray generator, it will reduce the external lead shielding weight and provide a net decrease in system weight. With the weight and size reductions accompanying the above indicated changes, and because the Unistrut steel frame structure was initially overdesigned, the weight of the system frame can be reduced significantly. As previously noted, the heavy (27 kg) forklift extension channels were added to provide a capability that was never needed. Removal of these channels along with the other above indicated changes would reduce the XMIS weight from 175 kg to around 100 kg.

Each detector assembly has a photomultiplier tube on each of its two ends for light collection. The location of these tubes makes them vulnerable to physical damage and does not yield the most efficient light collection in these long detectors. The replacement of the photomultiplier tubes with pin diodes along the detector length would yield a much more rugged detector assembly and improve the light collection. The latter will provide an improvement in the system imaging performance.

The rotating source beam collimator assembly on the x-ray generator provides for the side-to-side sweeping of the x-ray generator beam and for the relatively fast imaging capability of the XMIS. To cut down on cost, the collimator was made from PVC plastic sewer pipe and the beam slits were cut manually. The low cost belt assembly providing for the collimator rotation had a tendency to slip and jitter if the tension was not precisely adjusted. These limitations led to artifacts in the images, some of which could be compensated for. A carefully machined source beam collimator made from aluminum and a good drive assembly would provide a significant improvement in the XMIS imaging performance.

The length of the collimated detector collimators has a very significant effect on the quality of the collimated detector images. The optimum length increases with the depth of burial of the object that is being imaged. The collimator lengths on the XMIS were fixed. To achieve the effect of a change in length of the collimators, the whole assembly was raised or lowered relative to the ground using the four hand powered jacks attached to the system frame. This was extremely cumbersome and not very precise. Changes in collimator length of a cm are significant. Each of the detector collimators should have a small motor assembly that provides for fast, automatic changes in their length. Also, it is desirable to have the XMIS level relative to the ground that is being imaged. This task was accomplished by individually adjusting the four hand powered jacks. This process should be automated.

All of the above identified system modifications could be achieved within 6 months. There is one other modification that could yield a significant improvement in system performance. While the rotating source collimator provides for rapid side-to-side scanning, in order to achieve the back-to-front scanning, the XMIS x-ray generator travels on a set of rails using a motor driven worm screw. The need for this slow mechanical motion could be eliminated by constructing a multi-cathode x-ray generator with a single rod anode tube. The cathodes extend along the length of the tube. These cathodes do not have to be fired sequentially, but can be multiplexed and fired according to a preset order so as to obtain a series of beams to achieve the desired back-to-front scanning. In this way, a longer data collection time can be achieved for each cathode without suffering any interfering signal from a nearby cathode being fired quickly after. Work on such an x-ray generator has been done by Bio-Imaging Research, Inc. and development of such a generator for the XMIS system would take about a year. This will greatly increase the speed with which the system can image, should improve reliability and will also improve image quality. High resolution scanning of a 50 cm by 50 cm area which takes about a minute with the current XMIS should take no more than 20 to 30 s with a multi-cathode x-ray generator.

References

1. Campbell, S., and Jacobs, A., 'Detection of Buried Land Mines by Compton Backscatter Imaging," Nuclear Science and Engineering, 110, 417-424 (1992).
2. Watanabe, Y., Monroe, J., Keshavmurthy, S., Jacobs, A., and Dugan, E., "Computational Methods for Shape Restoration of Buried Objects in Compton Backscatter Imaging," *Nuclear Science and Engineering*, Vol 122, pp 55-67, 1996.
3. Wehlburg, J., Keshavmurthy, S., Watanabe, Y., Dugan, E., and Jacobs, A., "Image Restoration Techniques Using-Compton Backscatter Imaging for Detection of Buried Landmines," SPIE Proceedings on Detection Technologies for Mine and Minelike Targets, Paper 2496, pp 336-347, April, 1995.
4. Keshavmurthy, S., Dugan, E., Wehlburg, J., and Jacobs, A., "Analytical Studies of a Backscatter X-ray Imaging Landmine Detection System," SPIE Proceedings on Detection Technologies for Mine and Minelike Targets, Paper 2765-52, April, 1996.
5. Wehlburg, J., Keshavmurthy, S., Dugan, E., and Jacobs, A., "Experimental Measurement of Noise Removal Techniques for Compton Backscatter Imaging Systems as Applied to the detection of Landmines," SPIE Proceedings on Detection Technologies for Mine and Minelike Targets, Paper 2765-51, April, 1996.
6. Keshavmurthy, S., "Development of Lateral Migration Backscatter Radiography and Associated Image Enhancement Algorithms," Ph. D. Dissertation, University of Florida, Gainesville, Florida, August, 1996.
7. Wehlburg, J., Keshavmurthy, S., Dugan, E., and Jacobs, A., "Geometric Considerations Relating to Lateral Migration Backscatter Radiography (LMBR) as Applied to the Detection of Landmines," SPIE Proceedings on Detection and Remediation Technologies for Mine and Minelike Targets II, Vol. 3079, pp 384-393, Orlando, FL, April, 1997.
8. Wehlburg, J., I "Development of a Lateral Migration Radiography Image Generation and Object Recognition System," Ph. D. Dissertation, University of Florida, Gainesville, Florida, May, 1997.
9. Dugan, E., Keshavmurthy, S., Jacobs, A., and Wehlburg, J., "Monte Carlo Simulation of Lateral Migration Backscatter Radiography Measurements," ANS Trans., Vol 76, pp 140-142, June, 1997.
10. Jacobs, J., "Examination of Backscattered Radiation from X Rays Directed into Sand and Cross-Talk Between Adjacent Detector Systems," Masters Research Project, University of Florida, Gainesville, Florida, December, 1997.
11. Jacobs, A., Dugan, E., Howley, J., and Su, Z., "Landmine Detection/ Identification Using A New X-Ray Backscatter Imaging Technique," Third Symposium on Technology and the Mine Problem, Monterey, CA, April, 1998.
12. Dugan, E., Jacobs, A., Keshavmurthy, S., and Wehlburg, J.," Lateral Migration Radiography", Research in Nondestructive Evaluation, Vol 10, No. 2,pp 75-108, June, 1998.
13. Su, Z., "Concept and Application of a Vehicle-mounted Land Mine Detecton System Based on Lateral Migration Radiography," Masters Research Project, University of Florida, Gainesville, FL, August, 1998.
14. Howley, J., "Detailed Study of Lateral Migration Radiography Image, 5 Relevant to Landmine Detection," Masters Research Project, University of Florida, Gainesville, Fl, August, 1998.
15. Jacobs. A., Dugan, E., Howley, J., Su, Z., and Wells, C., "Detection/Identification of Landmines by Lateral Migration Radiography," Proceedings of Second International Conference on The Detection of Abandoned Mines, Institution of Electrical Engineers Publication No. 458,pp 152-156, Edinburg, UK, October, 1998.
16. Jacobs, J., Dugan, E., Jacobs, A., Lockwood, G., Shope, S., and Wehlburg, J., "Examination of The Crosstalk Between Adjacent X-Ray Generator Detector Systems," SPIE Proceedings on Detection and Remediation Technologies for Mines and Minelike Targets III, Vol 3392, pp 868-877, Orlando, Fl, April, 1998.
17. Su, Z, Howley, J., Jacobs, J., Dugan, E., and Jacobs, A., "The Discernibility of Landmines Using Lateral Migration Radiography," SPIE Proceedings on Detection and Remediation Technologies for Mines and Minelike Targets III, Vol 3392, pp 878-887, Orlando, Fl, April, 1998.
18. Wells, C., Su,Z., Moore, J., Dugan, E. and Jacobs, A., "Lateral Migration Radiography Measured Image Signatures For The Detection and Identification of Buried Landmines," SPIE Proceedings on Detection and Remediation Technologies for Mines and Minelike Targets IV, Vol 3710, pp 906-916, Orlando, FL, April, 1999.
19. Jacobs, A., Dugan, E., Moore, J., Su, Z., Wells, C., Ekdahl, D., and Brandy, J., "Imaging Subsurface Defects Using X-Ray Lateral Migration Radiography/A New Backscatter Technique," Proceedings of ASNT Conference on Real-Time Radioscopy and Digital Imaging, August, 1999.
20. Su, Z., Jacobs, A., Dugan E., Wells, C., Allard, A., Caniveau, G., "A Practical Land Mine Detection Confirmation System Based on X-ray Lateral Migration Radiography," Fifth Symposium on Technology and the Mine Problen4 Monterey, CA, April, 2000.

List of Publications and Reports

1. C. Wells, Z. Su, J. Moore, E. Dugan and A. Jacobs, "Lateral Migration Radiography Measured Image Signatures for the Detection and Identification of Buried Landmines," SPIE Proceedings on Detection And Remediation Technologies for Mines and Minelike Targets IV, Vol. 3710, pp 906-916, April, 1999.

2. Dugan, E. and Jacobs, A., "Lateral Migration Radiography Image Signatures for the Detection and Identification of Buried Landmines," Technical Report, ARO Grant No. DAAG-55-98-1-0400, University of Florida, Gainesville, Florida, January, 2000.

3. Su, Z., Jacobs, A., Dugan, E., Wells, C., Allard, A., Carriveau, G., "A Practical Land Mine Detection Confirmation System Based on X-ray Lateral Migration Radiography," Fifth Symposium on Technology and the Mine Problem, Monterey, CA, April,2000.

4. Wells, C., Su, Z., Allard, A., Salazar, S., Dugan, E., and Jacobs, A., "Suitability of Simulated Landmines for Detection Measurements Using X-ray Lateral Migration Radiography," SPIE Proceedings on Detection And Remediation Technologies for Mines and Minelike Targets V, Vol. 4038, pp , Orlando, FL, April, 2000.

5. Allard, A, Dugan, E. and Jacobs, A., "Image Processing Techniques for Lateral Migration Radiography Land Mine Images," Technical Report, ARO Grant Number DAAG-55-98-1-0400, University of Florida, Gainesville Florida, June, 2000.

6. Su, Z., Jacobs, A. , Dugan, E. and Ekdahl, D, "X-ray Lateral Migration Radiography System and Its Application in Land Mine Detection," Proceedings of SPIE 45th Annual Meeting, Symposium on Optical Science and Technology, San Diego, July, 2000.

7. Well, C. "Contributions To Measurement Systems for Land Mine Detection and Nondestructive Testing Using Lateral Migration Radiography," Masters Degree Research Project, University of Florida, Gainesville, Florida, August, 2000.

8. Su, Z., Jacobs, A., Dugan, E., Howley, J. and Jacobs, J. "Lateral Migration Radiography Application to Land Mine Detection, Confirmation and Classification," *Optical Engineering*, Vol. 39, No.9, pp 2472-2479, September, 2000.

9. Su, Zhong, "Fundamental Analysis and Algorithms for Development Of A Mobile Fast-Scan Lateral Migration Radiography System," Ph. D. Dissertation, University of Florida, Gainesville, Florida, August, 2001

10. Dugan, E. and Jacobs, A., "Lateral Migration Radiography Image Signatures for the Detection and Identification of Buried Land Mines," Final Technical Report, ARO Grant DAAG-55-98-1-0400, University of Florida, Gainesville, Florida, August, 2001.

11. Dugan, E., Jacobs, A., Houssay, L., Ekdahl, D, and Brygoo, S, "Development and Field Testing of a Mobile Backscatter X-ray Lateral Migration Radiography Land Mine Detection System," SPIE Proceedings on Detection and Remediation Technologies for Mines and Minelike Targets VII, Orlando, FL, April, 2002.

Scientific Personnel:

Edward T. Dugan, Ph.D., PI
Alan M. Jacobs, Ph.D., co-PI
Dan Ekdahl, Electronics Technician
Zhong Su, Graduate student
Christopher Wells, Graduate student
Anthony Allard, Graduate student
Laurent Houssay Graduate student
Robert Smith, Graduate student

Degrees Received:

Christopher Wells, Masters in Nuclear Engineering
Zhong Su, Ph.D. in Nuclear Engineering

Report of Inventions: None

Technology Transfer:

None yet. Because of the very successful imaging results on the vehicular test lanes at Fort A.P. Hill in October, 2001, it is expected that there should be significant interest, both here and outside the U.S., in developing LMR for both humanitarian and military mine detection applications, especially as a confirmation sensor.

In addition, as a result of this research, the idea of extending the principles of LMR to the detection of flaws and defects in materials and structures has received support from the DOE in the form of a 2 year $200 K research grant. Applications are to be investigated for which other techniques are unsatisfactory and where LMR, because of its unique features, may be expected to be successful. An example is in the detection of delaminations in certain carbon-carbon composites. Preliminary experiments and Monte Carlo simulations are very promising. Thus, a technology transfer may occur not only for land mine detection using LMR, but also for the detection of flaws and defects in materials and structures.

Appendix

Imaging Results Obtained on the Test Lanes
at Fort A.P. Hill Using the XMIS
Land Mine Detection System

List of Mine Types Imaged

M19: AT mine, square 33.2 x 33.2 cm and 9.4 cm height

VS1.6: AT mine, 22 cm diameter and 9 cm height

TM62M: AT mine, 32 cm diameter and 10.2 cm height

TM62P3: AT mine, 32 cm diameter and 12.5 cm height

M14: AP mine, 5.6 cm diameter and 4 cm height

PMN: AP mine, 11.2 cm diameter and 5.6 cm height

TS-50: AP mine, 9 cm diameter and 4.5 cm height

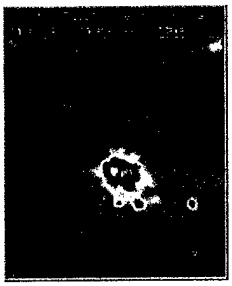

Front Collimated Detector

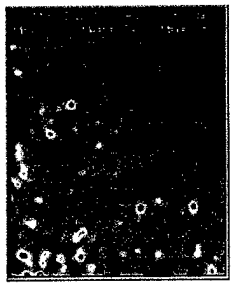

Uncollimated Detector

Back Collimated Detector

Image Set for TM62P3 AT Mine Buried Flush in Gravel

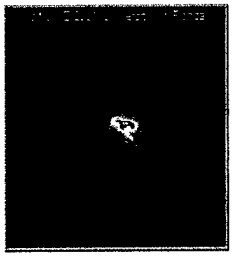

Processed Image

Ft. A.P. Hill
S&T Lane 19

This image set shows the front and back collimated and uncollimated detector images and the processed image for a TM62P3 anti-tank mine that is buried flush in gravel. This plastic mine shows clearly in all but the uncollimated detector image.

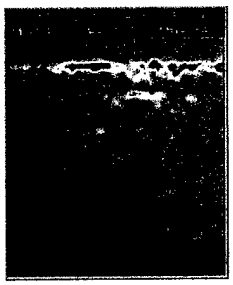

Front Collimated Detector

Uncollimated Detector

Back Collimated Detector

Image Set for TM62M AT Mine Buried Flush in Dirt

Processed Image

Ft. A.P. Hill
S&T Lane 19

This image set shows the front and back collimated and uncollimated detector images along with the processed image for a TM62M anti-tank mine buried flush in dirt. This is a metallic mine with a bakelite fuse. The mine is seen clearly in the latter three images and less clearly in the front collimated detector image. Because the mine is metallic, the mine gives a signal with an intensity decrease rather than an intensity increase as with a plastic mine.

Front Collimated Detector

Uncollimated Detector

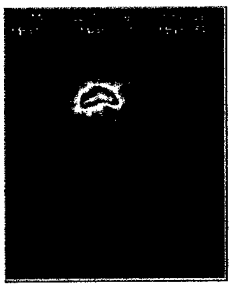

Back Collimated Detector

Image Set for TM62P3 AT Mine Buried Flush in Dirt

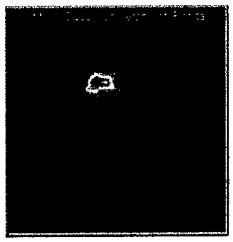

Processed Image

Ft. A.P. Hill
S&T Lane 19

This image set shows the front and back collimated and uncollimated detector images and the processed image for a TM62P3 anti-tank mine buried flush in dirt. The mine shows clearly in all but the uncollimated detector image and the quality is better than for the case when the mine is buried in gravel.

Front Collimated Detector

Uncollimated Detector

Back Collimated Detector

Image Set for M19 AT Mine with 1 Inch DOB in Dirt

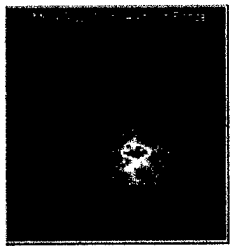

Processed Image

Ft. A.P. Hill
S&T Lane 19

This image set shows the front and back collimated and uncollimated detector images and the processed image for an M19 anti-tank mine with a 1 inch depth-of-burial (DOB) in dirt. The mine is clearly visible in all but the un-collimated detector image with the square shape showing best in the front collimated detector image. The square shape can also be seen in the processed image in the light magneta-colored region immediately surrounding the dark blue region.

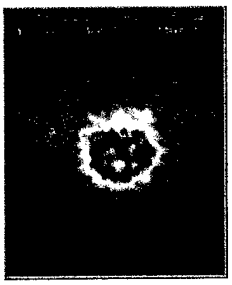

Front Collimated Detector

Uncollimated Detector

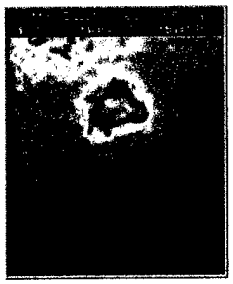

Back Collimated Detector

Image Set for VS1.6 AT Mine with 1 Inch DOB in Dirt

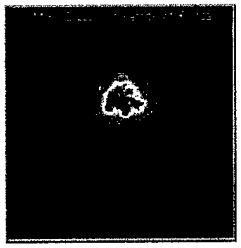

Processed Image

Ft. A.P. Hill
S&T Lane 19

This image set shows the front and back collimated and uncollimated detector images and the processed image for a VS1.6 anti-tank mine with a 1 inch DOB in dirt. The mine is clearly visible in all but the uncollimated detector image.

Front Collimated Detector

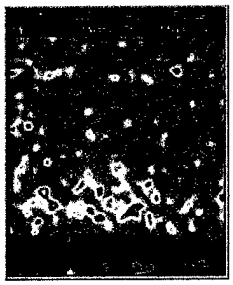

Uncollimated Detector

Back Collimated Detector

Image Set for M19 AT Mine with 1 Inch DOB in Gravel

Processed Image

Ft. A.P. Hill
S&T Lane 19

This image set gives the front and back collimated and uncollimated detector images and the processed image for an M19 anti-tank mine with a 1 inch DOB in gravel. The image quality is not as good as for the case when the mine is buried in dirt and the square shape is more difficult to discern. Nevertheless, the presence of an AT mine is very obvious.

Front Collimated Detector

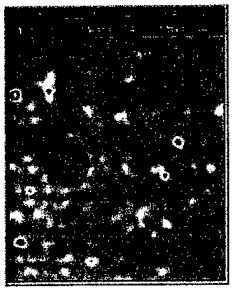

Uncollimated Detector

Back Collimated Detector

Image Set for M14 AP Mine with 1 Inch DOB in Dirt

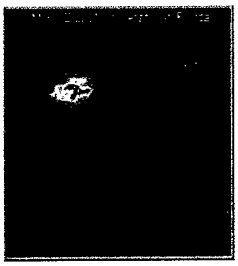

Processed Image

Ft. A.P. Hill
S&T Lane 19

This image set presents the front and back collimated and the uncollimated detector images and the processed image for an M14 anti-personnel mine with a 1 inch DOB in dirt. This small mine, with a diameter of only 2.2 inches, is easily seen in all but the uncollimated detector image.

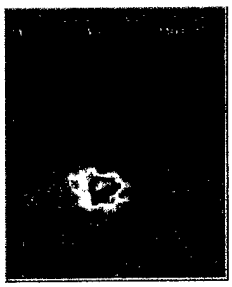

Front Collimated Detector

Uncollimated Detector

Back Collimated Detector

Image Set for M14 AP Mine with 0.5 Inch DOB in Dirt

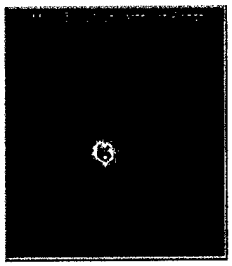

Processed Image

Ft. A.P. Hill
S&T Lane 19

This image set includes the front and back collimated and uncollimated detector images and the processed image for the small M14 mine with a 0.5 inch DOB in dirt. The mine is clearly visible in all but the uncollimated detector image.

Front Collimated Detector

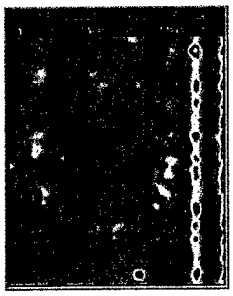

Uncollimated Detector

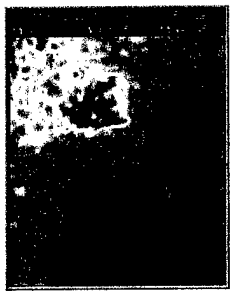

Back Collimated Detector

Image Set for M14 AP Mine with 2 Inch DOB in Dirt

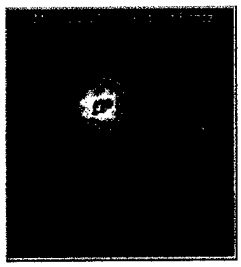

Processed Image

Ft. A.P. Hill
S&T Lane 19

This image set includes the front and back collimated and uncollimated detector images and the processed image for the small M14 mine with a 2 inch DOB in dirt. The mine is clearly visible in all but the uncollimated detector image where the mine presence is seen very faintly.

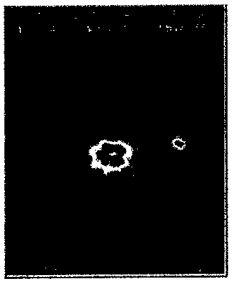

Front Collimated Detector

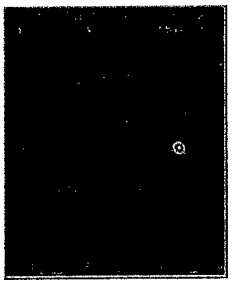

Uncollimated Detector

Back Collimated Detector

Image Set for TS50 AP Mine with 0.5 Inch DOB in Dirt

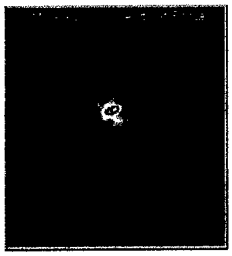

Processed Image

Ft. A.P. Hill
S&T Lane 19

This image set shows the front and back collimated and the uncollimated detector images and the processed image for a TS50 anti-personnel mine with a 0.5 inch DOB in dirt. This AP mine is larger than the M14, with a diameter of 3.5 inches. The mine shows clearly in all but the uncollimated detector image. A small surface object, like a pebble or golf tee position marker, appears to the right of the mine in all three detector images. It does not appear in the processed image because the uncollimated detector data has removed the surface "clutter."

Front Collimated Detector

Uncollimated Detector

Back Collimated Detector

Image Set for TS50 AP Mine with 2 Inch DOB In Grass & Dirt

Processed Image

Ft. A.P. Hill
S&T Lane 20

This image set includes the front and back collimated and uncollimated detector images and the processed image for a TS50 anti-personnel mine with a 2 inch DOB in grass and dirt. This is a difficult condition, but the mine is clearly visible on the bottom right in the processed image. It can also be seen in the back collimated detector image on the bottom right and with a bit more difficulty in the front collimated detector image, and even in the un-collimated detector image. A rock at the upper right center is responsible for the intensity decrease seen in all of the images.

Front Collimated Detector

Uncollimated Detector

Back Collimated Detector

Image Set for PMN AP Mine with 1 Inch DOB in Dirt

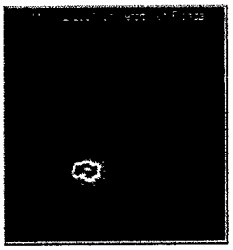

Processed Image

Ft. A.P. Hill
S&T Lane 19

This image set includes front and back collimated and uncollimated detector images and the processed image for a PMN anti-personnel mine with a 1 inch DOB in dirt. This mine, with a 4.4 inch diameter, is twice as large as the M14 AP mine. This mine is clearly visible in all but the uncollimated detector image.

Front Collimated Detector

Uncollimated Detector

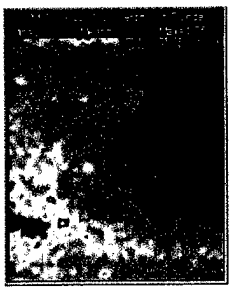

Back Collimated Detector

Image Set for GPR False Alarm Position #10

Processed Image

Ft A. P. Hill
S&T Lane 13

This image set includes the front and back collimated and uncollimated detector images and the processed image for GPR false alarm location #10. This position had one of the highest frequencies of correlated GPR false alarms. The back collimated detector shows a small, elongated amorphous high intensity area at the lower left, but there is no correlation with the other detector images. There is nothing mine-like in these images, just some soil inhomogeneities.

Front Collimated Detector

Uncollimated Detector

Back Collimated Detector

Image Set for GPR False Alarm Location #11

Processed Image

Ft. A.P. Hill
S&T Lane 13

This image set includes the front and back collimated and uncollimated detector images and the processed image. The back collimated detector image shows a high intensity area in the upper left, but there is no correlation with the other detector results. The back and front collimated detector images show amorphous low intensity areas at the bottom left and bottom center, respectively. There is nothing mine-like in these images, only soil inhomogeneities.

Front Collimated Detector

Uncollimated Detector

Back Collimated Detector

Image Set for Blank Area #5

Processed Image

Ft. A.P. Hill
S&T Lane 13

This image set includes the front and back collimated and uncollimated detector images and the processed image. There is nothing of note or nothing mine-like in any of these images, only soil irregularities.

Front Collimated Detector

Uncollimated Detector

Back Collimated Detector

Image Set for GPR False Alarm Location #20

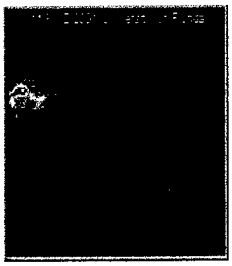

Processed Image

Ft. A.P. Hill
S&T Lane 13

This image set includes the front and back collimated and uncollimated detector images and the processed image. There is a high intensity area on the upper left in the back collimated detector image and a small, elongated high intensity area on the left in the front collimated detector which also shows in the processed image. This is not mine-like, but due to soil irregularities.

Front Collimated Detector

Uncollimated Detector

Back Collimated Detector

Image Set for GPR False Alarm Location #21

Processed Image

Ft. A.P. Hill
S&T Lane 13

This image set includes the front and back collimated and uncollimated detector images and the processed image. There is nothing mine-like in any of these images, only soil irregularities.

Front Collimated Detector

Uncollimated Detector

Back Collimated Detector

Image Set for Blank Area #6

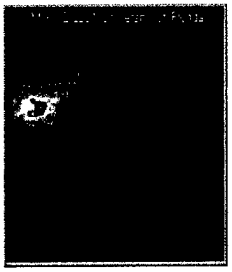

Processed Image

Ft. A.P. Hill
S&T Lane 13

This image set includes the front and back collimated and uncollimated detector images and the processed image. There are high intensity areas on the left and upper left in the front and back collimated detector images, respectively. The processed image contains a high intensity area in the upper left, which taken by itself, looks somewhat mine-like. The image set combination, however, suggests soil irregularities.

Front Collimated Detector

Uncollimated Detector

Back Collimated Detector

Image Set for Blank Area #10

Processed Image

Ft. A.P. Hill
S&T Lane 13

This image set includes the front and back collimated and uncollimated detector images and the processed image. There is a small elongated high intensity area on the lower left in the front collimated detector image and a large, amorphous high intensity area on the left in the back collimated detector image. The processed image shows a small distributed high intensity area on the left. This is not at all mine-like, but due to soil inhomogeneities.

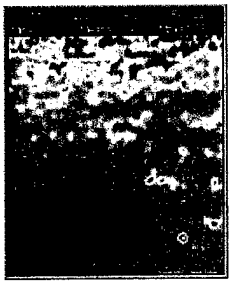

Front Collimated Detector

Uncollimated Detector

Back Collimated Detector

Image Set for GPR False Alarm Location #47

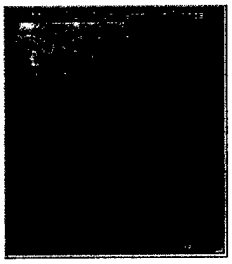

Processed Image

Ft. A.P. Hill
S&T Lane 13

This image set includes the front and back collimated and uncollimated detector images and the processed image. There is nothing of note and nothing mine-like in any of these images.

Front Collimated Detector

Uncollimated Detector

Back Collimated Detector

Image Set for GPR False Alarm Location #48

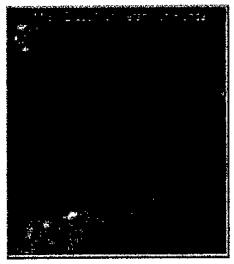

Processed Image

Ft. A.P. Hill
S&T Lane 13

This image set includes the front and back collimated and the uncollimated detector images and the processed image for GPR false alarm location #48. There is an elongated high intensity area on the lower left in the back collimated detector image, but no correlation with results from the other detectors. There is nothing mine-like in these images.

Front Collimated Detector

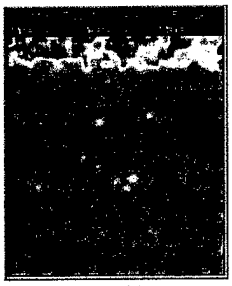

Uncollimated Detector

Back Collimated Detector

Image Set for GPR False Alarm Location #64

Processed Image

Ft. A.P. Hill
S&T Lane 13

This image set includes the front and back collimated and uncollimated detector images and the processed image for GPR false alarm location #64. There is nothing mine-like in any of these images, only soil irregularities.

Front Collimated Detector

Uncollimated Detector

Back Collimated Detector

Image Set for Blank Area #16

Processed Image

Ft. A.P. Hill
S&T Lane 13

This image set includes the front and back collimated and uncollimated detector images and the processed images for blank area #16. There is nothing that resembles a mine in these images. The front and back collimated detector images and the processed image show a horizontal strip of high intensity while the uncollimated detector image shows a horizontal strip at this location of low intensity. This strip is due to a ridge in the soil.

Front Collimated Detector

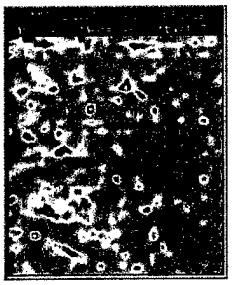

Uncollimated Detector

Back Collimated Detector

Image Set for GPR False Alarm Location #69

Processed Image

Ft. A.P. Hill
S&T Lane 13

This image set includes the front and back collimated and uncollimated detector images and the processed image for GPR false alarm location #69. There is nothing mine-like in any of these images, only soil inhomogeneities.

Front Collimated Detector

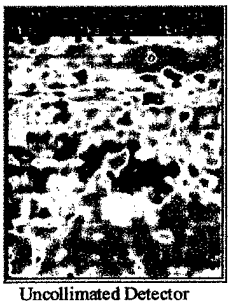

Uncollimated Detector

Back Collimated Detector

Image Set for GPR False Alarm Location #70

Processed Image

Ft. A.P. Hill
S&T Lane 13

This image set includes the front and back collimated and uncollimated detector images and the processed image for GPR false alarm location #70. There is a large, amorphous high intensity area in the back collimated detector image. There is nothing mine-like in these images, only soil inhomogeneities.

Front Collimated Detector

Uncollimated Detector

Back Collimated Detector

Image Set for GPR False Alarm Location #77

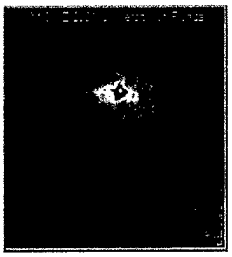

Processed Image

Ft. A.P. Hill
S&T Lane 13

This image set presents the front and back collimated and uncollimated detector images and processed image for GPR false alarm location #77. There are high intensity areas in the center and upper center of the front and back collimated detector images, respectively. The correlated high intensity area in the processed image has a signature that is similar to that of a deep buried (~2 inches) AP mine. Of all the GPR false alarm locations, this site had the most mine-like combination of LMR images.

Front Collimated Detector

Uncollimated Detector

Back Collimated Detector

Image Set for GPR False Alarm Location #83

Processed Image

Ft. A.P. Hill
S&T Lane 13

This image set includes the front and back collimated and uncollimated detector images and the processed image for GPR false alarm #83. There is a large, scattered high intensity area in both the front and back collimated detector images. There is a small, correlated, mild high intensity area at the top center of the processed image which, by itself, could be considered somewhat mine-like. The collection of images, however, points towards soil irregularities as the source of these high intensity areas.

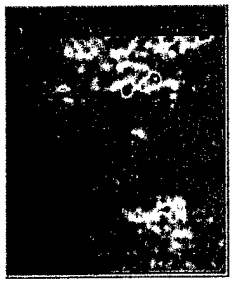

Front Collimated Detector

Uncollimated Detector

Back Collimated Detector

Image Set for Blank Area #24

Processed Image

Ft. A.P. Hill
S&T Lane 13

This image set includes the front and back collimated and uncollimated detector images and the processed image for blank area #24. There is a high intensity area at the top left of the back collimated detector image that is not correlated with other detector results. There is a small, weak high intensity area just below and just right of center in the back collimated detector image that is correlated with a similar area in the front collimated detector image. The processed image shows this small high intensity area which is not at all mine-like. This area is due to a wooden golf tee marker that was inadvertently left in place during the imaging.

Front Collimated Detector

Uncollimated Detector

Back Collimated Detector

Image Set for GPR False Alarm Location #96

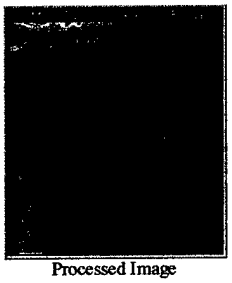

Processed Image

Ft. A.P. Hill
S&T Lane 13

This image set includes the front and back collimated and uncollimated detector images and the processed image for GPR false alarm location #96. There is nothing mine-like in any of these images, only soil irregularities.

Front Collimated Detector

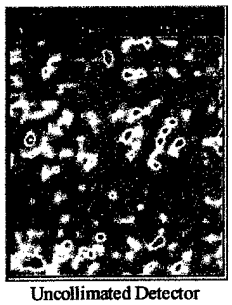

Uncollimated Detector

Back Uncollimated Detector

Image Set for GPR False Alarm Location #105

Processed Image

Ft. A.P. Hill
S&T Lane 13

This image set presents the front and back collimated and uncollimated detector images and processed image for GPR false alarm location #105. There is nothing mine-like in any of these images; only soil irregularities.

Front Collimated Detector

Uncollimated Detector

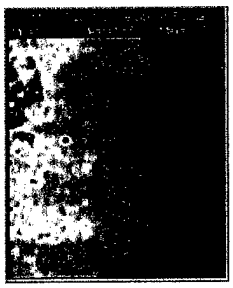

Back Collimated Detector

Image Set for GPR False Alarm Location # 109

Processed Image

Ft. A.P. Hill
S&T Lane 13

This image set includes the front and back collimated and uncollimated detector images and the processed image for GPR false alarm location #109. There is a mild high intensity area in the upper center of the front collimated detector image and a high intensity area on the left in the back collimated detector image, but no correlation. There is nothing mine-like in these images.

Front Collimated Detector

Uncollimated Detector

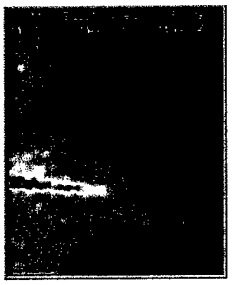

Back Collimated Detector

Image Set for GPR False Alarm Location #110

Processed Image

Ft. A.P. Hill
S&T Lane 13

This image set includes the front and back collimated and uncollimated detector images and the processed image for GPR false alarm location #110. There is a horizontal, high intensity strip on the left in the back collimated detector image which appears weakly in the uncollimated detector image and very faintly in the front collimated detector image. This is due to a soil ridge. Image correlation for this region yields a a small, irregular high intensity area on the left in the processed image, but nothing that is mine-like.

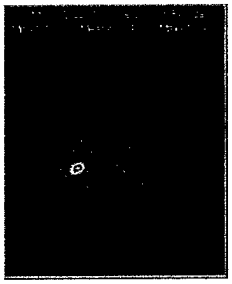

Front Collimated Detector

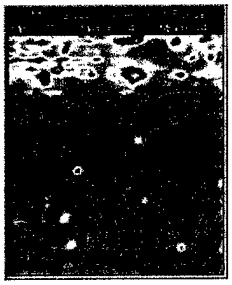

Uncollimated Detector

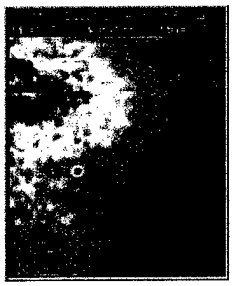

Back Collimated Detector

Image Set for GPR False Alarm Location #116

Processed Image

Ft. A.P. Hill
S&T Lane 13

This image set includes the front and back collimated and uncollimated detector images and processed image for GPR false alarm location #116. There is an irregular high intensity area in the center of the front collimated detector image and a large high intensity area on the left in the back collimated detector image. The processed image shows a correlated, irregular high intensity area which, by itself, could be considered vaguely mine-like. The image combination, however, does not suggest a mine, but soil inhomogeneities

Front Collimated Detector

Uncollimated Detector

Back Collimated Detector

Image Set for Rock in S&T Lane 13

Processed Image

Ft. A.P. Hill
S&T Lane 13

This image set includes the front and back collimated and uncollimated detector images and processed image for a rock that was located between GPR false alarm locations #116 and #118. The rock had surface dimensions of about 6 inches by 4 inches and an unknown size below the surface. The rock shows as a high intensity area in the uncollimated detector and processed images and as a low intensity area in the front and back collimated detector images. This rock, whose surface was slightly above the soil surface, is seen to cast a shadow (high intensity area) in the front and back collimated detector images.

Front Collimated Detector

Uncollimated Detector

Back Collimated Detector

Image Set for GPR False Alarm Location #118

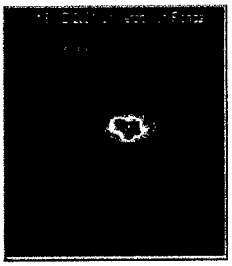

Processed Image

Ft. A.P. Hill
S&T Lane 13

This image set includes the front and back collimated and uncollimated detector images and processed image for GPR false alarm location #118. There is an oval high intensity area in the front collimated detector image that correlates with a similar high intensity area in the back collimated detector image. The processed image shows an oval high intensity area that looks mine-like. However, the uncollimated detector image shows a clear low intensity area at this location. This combination of image signatures is representative of an area of decreased soil density rather than of a mine.

Front Collimated Detector

Uncollimated Detector

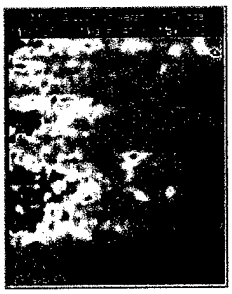

Back Collimated Detector

Image Set for GPR False Alarm Location # 122

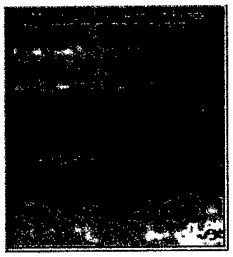

Processed Image

Ft. A.P. Hill
S&T Lane 13

This image set includes the front and back collimated and uncollimated detector images and the processed image for GPR false alarm location #122. There is nothing mine-like in any of these images, only soil inhomogeneities.

Front Collimated Detector

Uncollimated Detector

Back Collimated Detector

Image Set for GPR False Alarm Location #128

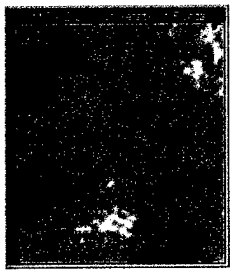

Processed Image

Ft. A.P. Hill
S&T Lane 13

This image set includes the front and back collimated and uncollimated detector images and the processed image for GPR false alarm location #128. There is a high intensity area at the bottom of the front collimated detector image that correlates mildly with a large, high intensity area that includes a high intensity strip near the bottom center of the back collimated detector image. The result is a weak, irregular high intensity area at the bottom of the processed image. There is nothing mine-like.

Front Collimated Detector

Uncollimated Detector

Back Collimated Detector

Image Set for GPR False Alarm Location #130

Processed Image

Ft. A.P. Hill
S&T Lane 13

This image set includes the front and back collimated and uncollimated detector images and the processed image for GPR false alarm location #130. The front and back collimated detector images show some fairly large, amorphous high intensity areas with the latter being of higher intensity. The processed image shows very mild correlation and a weak high intensity area at the top of the image that does not look mine-like. The high intensity areas are the result of soil irregularities.

Front Collimated Detector

Uncollimated Detector

Back Collimated Detector

Image Set for GPR False Alarm Location #139

Processed Image

Ft. A.P. Hill
S&T Lane 13

This image set includes the front and back collimated and uncollimated detector images and the processed image for GPR false alarm location #139. There is nothing mine-like in any of these images, only soil irregularities.

Front Collimated Detector

Uncollimated Detector

Back Collimated Detector

Image Set for GPR False Alarm Location #140

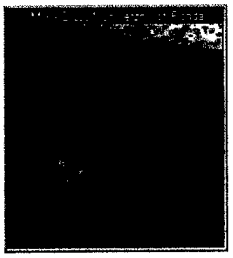

Processed Image

Ft. A.P. Hill
S&T Lane 13

This image set includes the front and back collimated and the uncollimated detector images and the processed image for GPR false alarm location #140. The back collimated detector image shows a large, amorphous high intensity area. There is a weaker high intensity area in the front collimated detector image in this region and the processed image shows a weak high intensity area in this region. Close examination of the uncollimated detector shows a very small low intensity spot at this location. This combination indicates a region of reduced soil density.

Front Collimated Detector

Uncollimated Detector

Back Collimated Detector

Image Set for GPR False Alarm Location #141

Processed Image

Ft. A.P. Hill
S&T Lane 13

This image set includes the front and back collimated and uncollimated detector images and processed image for GPR false alarm location #141. There is nothing mine-like in any of these images, only soil inhomogeneities.

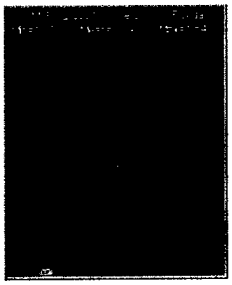

Front Collimated Detector

Uncollimated Detector

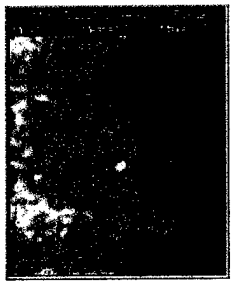

Back Collimated Detector

Image Set for GPR False Alarm Location #159

Ft A.P. Hill
S&T Lane 13

This image set includes the front and back collimated and uncollimated detector images and the processed image for GPR false alarm location #159. There is nothing mine-like in any of these images, only soil irregularities.

Front Collimated Detector

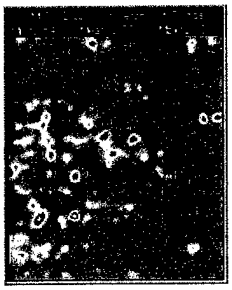

Uncollimated Detector

Back Collimated Detector

Image Set for GPR False Alarm Location #172

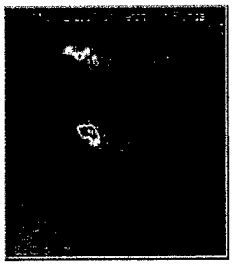

Processed Image

This image set includes the front and back collimated and uncollimated detector images and the processed image for GPR false alarm location #172. There is a small high intensity area near the center of the back collimated detector image and a pair of small high intensity areas above and below this location in the front collimated detector image. The processed image also contains two small high intensity areas, the lower one of which could conceivably be due to a deep-buried (~2 inch) AP mine. But because the uncollimated detector image has a clear low intensity area at this location, this feature is more likely due to a region of reduced density in the soil.